TITLE: T6SS-mediated competition by *Stenotrophomonas rhizophila* shapes seed-borne bacterial communities and seed-to-seedling transmission dynamics

Running Title: T6SS impact on transmission of seed bacterial communities

AUTHORS:

Tiffany Garin[1], Agathe Brault[1], Coralie Marais[1], Martial Briand[1], Anne Préveaux[1], Marie Simonin[1], Matthieu Barret[1], Alain Sarniguet[1]

AFFILIATION:

[1]Univ Angers, Institut Agro, INRAE, IRHS, SFR QUASAV, F-49000 Angers, France

ABSTRACT

Seeds harbor diverse microbial communities important for plant growth and health. During germination, seed exudation triggers intense microbial competition, shaping the communities transmitted to seedlings. This study explores the role of the bacterial type VI secretion system (T6SS)-mediated interference competition in seed microbiota transmission to seedlings. Distribution of T6SS within 180 genome sequences of seed-borne bacterial strains enabled the construction of SynCom with different levels of phylogenetic diversity and T6SS richness. These SynComs were inoculated with *Stenotrophomonas rhizophila* CFBP13503, a bacterial strain which possesses a T6SS active *in vitro* and *in planta*. SynComs compositions were compared *in vitro* with CFBP13503 wild-type strain or its isogenic T6SS-deficient mutant. Additionally, the effects of T6SS on the whole bacterial community dynamics during seed-to-seedling transmission were examined following seed-inoculation. The T6SS of *S. rhizophila* CFBP13503 targeted a large number of bacteria belonging to 5 different families The phylogenetic proximity and metabolic overlap of preys with CFBP13503 partly explains the sensitivity phenotype observed. The T6SS of CFBP13503 modulates the abundance of a few specific bacterial taxa during seed-to-seedling transmission depending on seed microbial initial inoculation and plant stage. Depending on the sensitivity of the co-inoculated competitors, the T6SS can provide a competitive advantage to CFBP13503, resulting in an increase in population size.

Importance: The high prevalence of T6SS in seed-borne bacteria supports the importance of T6SS-mediated competition for seed microbiota assembly. *In vitro*, *S. rhizophila* CFBP13503 T6SS exerts a strong impact on bacterial community dynamics. The susceptibility to T6SS increases with the phylogenetic and metabolic proximity of bacteria to CFBP13503, suggesting an influence of interspecies trophic patterns in T6SS-mediated competitions. *In planta* and in soil, CFBP13503 T6SS influences specific bacterial taxa, leading to shifts in bacterial interactions and distinct community dynamics. T6SS-mediated competition plays a pivotal role in shaping seed bacterial communities and the dynamics of seed-to-seedling transitions.

INTRODUCTION

Seeds serve as a vector for the dissemination of numerous plant-associated microorganisms (1). While seeds are often considered as the starting point for the assembly of plant microbiota (2), the percentage of seed-borne microorganisms successfully transmitted to seedlings is quite variable (3–7). These variations in seedling transmission of seed-borne microbes may be attributed to competition with soil-borne taxa for seedling colonization (8). This competition between microorganisms is the result of the exudation of numerous molecules during seed imbibition, which creates a specific habitat - the spermosphere (9). Like other habitats (i.e. rhizosphere and phyllosphere), the nature and quantities of exudates is an important driver of microbial community composition (10). This is perhaps even more striking within the spermosphere since the plant defense responses appear to be not induced during germination (11, 12). Hence microbial competition is probably a key factor for successful seedling colonization.

Microbial competition could be broadly divided into exploitative and interference competitions (13). The former is based on the rapid and efficient use of resources, a strategy used by copiotroph (14). High relative abundance of copiotrophic bacterial taxa have been reported in seedlings (15, 16) and spermospheres (10) of different plant species. These observations suggested that this life history strategy is important for seed to seedling transmission. In contrast to exploitative competition, interference competition relies on limiting the access of other microorganisms to resources through the production of antimicrobial compounds (13). Among the wide range of mechanisms used to inhibit microbial growth, contact-dependent mechanisms based on the Type VI Secretion System (T6SS) have been well studied (17, 18).

T6SS is a contractile nanomachine found in many gram-negative bacteria. T6SSs are categorized into four subtypes: T6SS^{i} mainly found in Proteobacteria and subdivided into subgroups i1 to i5 (19–22), T6SS^{ii} specific to *Francisella* (23, 24), T6SS^{iii} present in Bacteroidetes (25), and T6SS^{iv} found in *Amoebophilus asiaticus* (26). T6SS is used by bacteria to inject effectors directly into prokaryotic or eukaryotic cells and, for few, in proximal environments (27). Toxic effectors are associated with the arrow of the system composed of the Hcp tube capped with the VgrG/PAAR spike. Surrounded by a contractile sheath, the arrow is propelled by mechanical force, allowing the delivery of toxic effectors into the target cell. Effectors are associated with cognate immunity proteins to prevent cell self-intoxication (28, 29). Other non-immune defense mechanisms can also provide protection against T6SS attack, such as spatial separation and rapid growth, general stress responses, and the presence of physical barriers preventing T6SS from reaching its target (30, 31).

Competition-relatedness theory postulates that competition should be more intense between closely related species that may share similar functions and substrate affinities. Antagonism experiments between bacterial strains from a diverse range of phyla confirm this theory during production of diffusible compounds in synthetic media (32). However, we can ask whether this theory also works with other bacterial weapons such as contact-dependent growth inhibition systems like T6SS? To investigate this theory extension, we rely on the strong T6SS-mediated antibiosis provided by a *Stenotrophomonas rhizophila* strain (CFBP13503) *in vitro* against the phytopathogenic bacterium *Xanthomonas campestris* pv. *campestris* 8004 (Xcc8004) (33). *S. rhizophila* CFBP13503 is a seed-borne bacterial strain isolated from radish (34) that displays a high transmission rate from seed to seedling (35) and limits Xcc8004 populations *in planta* in a T6SS-manner (33). In the present work, the wild-type strain of *S. rhizophila* CFBP13503 and its isogenic T6SS-deficient mutant were inoculated in synthetic communities (SynComs) of different phylogenetic diversity in a culture medium. If competition-relatedness theory applies to our study model, then we anticipate a greater effect of CFBP13503 T6SS in communities with low phylogenetic diversity compared to those with high phylogenetic diversity. This experimental system also enabled the estimation of the range of bacterial prey targeted by the *S. rhizophila* T6SS *in vitro*. Finally we deployed the SynCom approach *in planta* for analyzing the significance of *S. rhizophila* T6SS during seed to seedling transmission.

96

MATERIALS AND METHODS

Bacterial strain collection from seed and genome sequencing

Bacterial isolates were collected from seed lots of radish (*Raphanus sativus*), winter oil seed rape (*Brassica napus*) and common bean (*Phaseolus vulgaris*) (**Table S1**). For each seed lot, 500 to 1000 seeds were soaked in 4 ml of PBS supplemented with Tween20 (0.05% v/v), for 2h30 (radish and rapeseed) and 16h (bean) at 4°C under constant agitation. Suspensions were serially diluted and plated on Tryptic Soy Agar 1/10 (17 $g.L^{-1}$ tryptone, 3 $g.L^{-1}$ soy peptone, 2.5 $g.L^{-1}$ glucose, 5 $g.L^{-1}$ NaCl, 5 $g.L^{-1}$ K2HPO4 and 15 $g.L^{-1}$ agar) supplemented with cycloheximide (50 $\mu g.mL^{-1}$). After 7 days incubation at 18°C, 200 to 300 colonies per seed lot were subcultured from several Petri dishes of different colony density (10 to 150) into 96-well plates containing 200 µL Tryptic Soy Broth. After 5 days' incubation of the plates at 18°C with constant agitation (70 rpm), 10 µL of bacterial suspension was transferred to 90 µL of sterile water for subsequent PCR amplification. 190 µL sterile 80% glycerol was added to each well of the remaining bacterial suspensions and the plates were stored at -80°C. Molecular typing of each bacterial isolate was conducted with a portion of the *gyrB* gene following the procedure described by Armanhi et al. (2016) (36). For the detailed procedure also applied to bacterial community metabarcoding see below the "*gyrB* amplification sequencing" section.

A total of 180 purified bacterial isolates were subjected to Illumina HiSeq 4000 PE150 sequencing. These isolates were chosen by comparing their *gyrB* haplotypes with *gyrB* sequences previously obtained on seed samples. All genome sequences were assembled with SOAPdenovo 2.04 (37) and VELVET 1.2 (38).

Phylogenetic analysis, prediction of functional trait and assessment of T6SS distribution

Phylogenomics of the 180 genomes of bacterial strains isolated from seeds and seedlings of *B. napus*, *P. vulgaris* and *R. sativus* (**Table S1**) was performed using the following procedure (39). Briefly, marker genes were extracted with AMPHORA2 (40). A total of 24 single-copy genes detected in all genome sequences were selected for subsequent phylogenetic analysis. Sequence alignment was performed with MUSCLE. Alignments were concatenated and a maximum likelihood phylogenetic tree was built with RAxML v8 (41). Phylogenetic tree was

displayed and annotated with iTol v6.8 (42). The pairwise phylogenetic distances between *S. rhizophila* CFBP13503 and each bacterial strain was computed with the cophenetic.phylo function of the ape v5.7.1 package (doi:10.1093/bioinformatics/bty633).

Prediction of functional traits from bacterial genomes was performed with microTrait v1.0.0 (43). Resource acquisition traits (at granularity 3) were selected. The resource overlap between CFBP13503 and bacterial strains was calculated by dividing the number of shared resource traits (between CFBP13503 and each strain) by the total number of resource traits of CFBP13503.

Detection of T6SS within genome sequences is based on the search for 10 Clusters of Orthologous Groups (COG3515, COG3516, COG3517, COG3518, COG3519, COG3520, COG3521, COG3522, COG3455, COG3523) specifics to T6SS (Barret et al., 2013). Classification of T6SS was performed through analysis of TssB protein sequences (COG3516) with the SecReT6 database v3 (44).

In vitro SynCom confrontation assays

Forty-five bacterial strains isolated from seeds of radish and rapeseed were used to build SynComs (**Table S2, Fig. 1A** and **Fig. 1B**). These strains possess unique *gyrB* Amplicon Sequence Variants (ASVs) and are representative of the range of variable prevalence in seed microbiota (**Fig. 1b**). Five SynComs with different phylogenetic diversity and number of T6SS loci were constructed (**Fig. 1C** and **Fig. 1D**). Each of these 5 SynComs were supplemented with Xcc8004, a strain previously identified as sensitive to the T6SS of *S. rhizophila* CFBP13503 (33). Finally, each SynCom was mixed with either the strain *S. rhizophila* CFBP13503 or the isogenic T6SS deficient-mutant Δ*hcp* (33).

To construct each SynCom, bacterial strains were cultured overnight in 10 ml of TSB10% at 28°C under constant agitation (150 rpm). Overnight cultures were centrifuged (4,000 g, 8 min) and the resulting pellets were resuspended in sterile water at a bacterial concentration of 5.10^8 cells.ml^{-1}. Bacterial concentrations were determined according to correspondence between OD_{600nm} and number of colony-forming units (CFUs). SynCom were obtained by mixing equivalent volumes of each bacterial suspension (n=10). These initial SynCom mixtures were then combined with equal volumes of *S. rhizophila* CFBP13503 or the isogenic T6SS deficient-mutant, resulting in confrontation mixtures containing 50% of CFBP13503 and 50% of the other SynCom members. Twenty µl drops (n=10) were spotted on TSA10% and incubated at 28°C for 6 and 24 hours (4 repetitions per SynCom). Simultaneously, 500 µl of each initial confrontation mixture were centrifuged (11,000 g, 5 min) and the resulting

pellets were stored at -80°C for subsequent DNA extraction. After 6 and 24 hours of confrontation, inoculated spots were resuspended in 1.5 ml and 5 ml of sterile water, respectively. 500 µl of these cell suspensions were centrifuged (11,000 g, 5 min) and the pellets were stored at -80°C. DNA extraction was performed with the Wizard® Genomic DNA Purification Kit (Promega) using supplier recommendations.

The relative abundance of each bacterial strain was assessed using *gyrB* amplicon sequencing (see below). To evaluate the enrichment or depletion of bacterial strains in response to the T6SS of *S. rhizophila* CFBP13503, we use the following formula $\log_2[(RA_{6h}/RA_{0h})_{WT} / (RA_{6h}/RA_{0h})_{\Delta hcp}]$, which measures change in relative abundance (RA) between the initial (0h) and 6-hour time points (6h) in presence (WT) and absence (Δ*hcp*) of functioning T6SS.

Pairwise confrontation assay *in vitro*

Change in strain abundance following confrontation with CFBP13503 WT or the isogenic T6SS-deficient mutant was also measured by pairwise confrontation assays. Twenty phylogenetically distinct strains were selected. Spontaneous rifampicin-resistant (Rif^R) variants were generated for each strain. Variants with no growth differences (TSB10%, 24h, 500 rpm) from the wild-type strains were selected .

S. rhizophila CFBP13503, CFBP13503Δ*hcp* and the selected Rif^R bacterial strains were cultured overnight in 10 mL of TSB10% (28°C, 150 rpm). Overnight cultures were centrifuged (4,000 g, 8 min) and the resulting pellets were resuspended in sterile water at an OD_{600nm} of 0.5. One hundred µl of Rif^R bacterial suspension and 100 µl of *S. rhizophila* CFBP13503 (WT or Δ*hcp*) suspensions were mixed. As a control, 100 µl of bacterial suspensions were mixed with 100 µL of sterile water. Three individual 20 µl drops were deposited on TSA10% and incubated at 28°C for 6 hours and 24 hours. Inoculated spots were resuspended in 2.5 ml of sterile water, serial diluted and plated on TSA10% either containing spectinomycin (50 $\mu g.ml^{-1}$) and ampicillin (100 $\mu g.ml^{-1}$) for *S. rhizophila* or rifampicin (50 $\mu g.ml^{-1}$) for the Rif^R bacterial strains. Changes in CFU abundances were considered as significant at a p-value < 0.05 (Wilcoxon test).

Impact of the T6SS of CFBP13503 on bacterial communities' compositions during seedling transmission

The impact of *S. rhizophila* CFBP13503 T6SS on seedling transmission was evaluated by inoculating sterilized radish seeds (*Raphanus sativus* var. Flamboyant5) with *S. rhizophila* CFBP13503 WT or the isogenic T6SS-deficient mutant. Both strains were inoculated on radish seeds alone or in the presence of two SynComs, SCA and SCB (**Fig. 1A** and **Fig. 1B**). SCA was composed of 4 T6SS-sensitive strains (CFBP8803, CFBP13510, CFBP13709 and CFBP13725), whereas SCB was assembled with 2 T6SS-sensitive strains (CFBP8753 and CFBP13505) and 2 T6SS-resistant strains (CFBP13531 and CFBP13644). The relative abundance of each strain was measured using *gyrB* amplicon sequencing on 8 individual seeds just before sowing (0 dpi), 8 individual germinated seeds after sowing (1 dpi) and 8 individual seedlings (5 dpi).

Bacterial suspensions were prepared at a concentration of 10^9 cells.ml^{-1} from 24h TSA10% plates. SynComs were obtained by mixing equivalent volumes of each bacterial suspension (n=4). These initial SynCom mixtures were then combined with equal volumes of *S. rhizophila* CFBP13503 or the isogenic T6SS deficient-mutant, resulting in mixtures containing 50% of *S. rhizophila* and 50% of the other SynCom members. In addition, both *S. rhizophila* strains (WT or Δ*hcp*) were inoculated alone on seeds at a concentration of 10^9 cells.ml^{-1} mixed with an equivalent volume of sterile water.

Radish seeds were surface-sterilized using the protocol employed in Simonin et al., 2023 (35). Briefly, seeds were sonicated (40 Hertz, 1 min), then immersed in 96° ethanol (1 min), 2.6% sodium hypochlorite (5 min), 96° ethanol (30 s) and rinsed three times with sterile water. Sterilized seeds were dried (30 min) on sterile paper and distributed in subsamples of 60 seeds. These subsamples were inoculated with: sterile water (uninoculated control), CFBP13503WT, CFBP13503*Δhcp,* SCA+CFBP1503WT, SCA+CFBP13503*Δhcp*, SCB+CFBP13503WT, SCB+CFBP13503Δ*hcp* and incubated at 20°C (70 rpm, 15 min) before being dried on sterile paper (15 min). Forty seeds from each condition were subsequently sown in seedling cell trays containing unsterile, pre-moistened potting soil (Traysubstrat 75/25, Klasmann-Deilmann, Germany) at a depth of 5mm. The trays were then placed in a growth chamber (photoperiod: 16h/8h, 20°C). Eight remaining seeds were individually resuspended in 1.5 ml of sterile water by vortexing for 30 seconds. Five hundred µl were stored at -80°C and 200 µl were diluted and plated on TSA10% (total bacteria) and TSA10%+Amp100+Spe50 (selective medium for CFBP13503). Eight germinated seeds (1

dpi) per condition were individually placed in sterile bags containing 2 ml of sterile water and 500 µl and 200 µl of the resulting suspensions were stored at -80°C and diluted and plated, respectively. Eight seedlings per condition were collected at 5 dpi. The aerial parts and the roots were separated, removing as much adhering soil as possible. Each part was placed individually in sterile bags with 2 mL of sterile water and processed like germinated seeds. At each time point (0, 1 and 5 dpi) soil samples were collected and stored at -80°C.

gyrB amplicon sequencing

Community profiling was performed through *gyrB* amplicon sequencing following the procedure described earlier (15). Briefly the first PCR step was performed with the gyrB_aF64/gyrB_aR553 primer set using the AccuPrimeTM Taq DNA Polymerase (Invitrogen, Carlsbad, California, USA). PCR products were purified with Sera-MagTM (Merck, Kenilworth, New Jersey). Illumina adapters and barcodes were added with a second PCR. PCR products were purified and pooled at equimolar concentration. The pooled amplicon library was quantified with the KAPA Library Quantification Kit (Roche, Basel, Switzerland). Amplicon library was mixed with 5% of PhiX and sequenced with four MiSeq reagent kits v3 600 cycles (Illumina, San Diego, California, USA). A blank extraction kit control, a PCR-negative control and PCR-positive control (*Lactococcus piscium* DSM 6634, a fish pathogen that is not plant-associated) were included in each PCR plate. The raw amplicon sequencing data are available on the Sequence Read Archive (SRA) with the accession number PRJNA1127244.

Sequence analyses of *gyrB* were performed as follows. Primer sequences were removed with cutadapt 2.7 (45) and trimmed fastq files were processed with DADA2 v 1.10 (46). The following parameters were employed for sequence filtering and trimming: maxN=0, maxEE=c(2,2), truncQ=3. The truncLen parameter was adapted for each sequencing run (25th percentile < Q30). Chimeric sequences were removed with the removeBimeraDenovo function of DADA2. Post-clustering curation of Amplicon Sequence Variant (ASV) was performed with LULU v 0.1.0 (47) at a similarity threshold of 99%. Taxonomic affiliation of each ASVs was performed with a naive Bayesian classifier (48) with our in-house *gyrB* database (train_set_gyrB_v5.fa.gz) available upon request. Unassigned sequences at the phylum level and *parE* sequences (a *gyrB* paralog) were filtered. The identification of sequence contaminants was assessed using decontam (49) v 1.8.0 at a threshold of 0.3.

Diversity analyses were conducted with PhyloSeq 1.40.0 (50). Alpha-diversity indexes (richness and Pielou's evenness) were calculated after rarefaction of 2,700 (*in vitro* assay) and 5,000 (*in planta* assay) reads per sample. Changes in bacterial phylogenetic composition were estimated with weighted UniFrac distances (51). A permutational multivariate analysis of variance was performed with the adonis2 function of vegan 2.6.4. Changes in relative abundance was assessed with the microViz v 0.10.5 package (52) using a beta-binomial regression model provided in the corncob v 0.3.1 package (53). Taxa were filtered at a minimum prevalence threshold of 0.2. Changes in relative abundances were considered as significant at a p-value < 0.05.

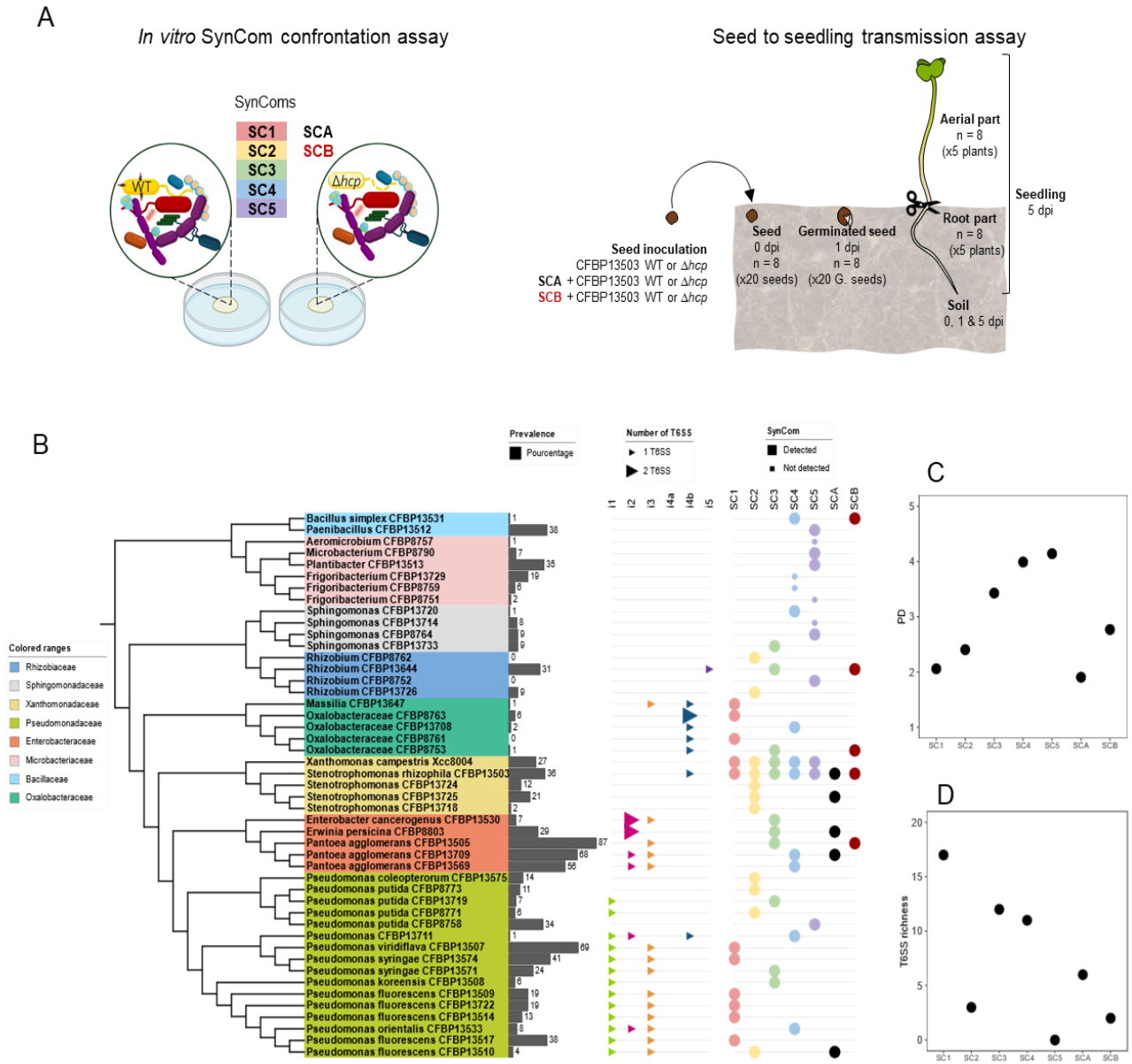

Figure 1. Overview of experimental designs and strain sensitivity to T6SS. The impact of the T6SS of *S. rhizophila* CFBP13503 on the composition of synthetic communities (SynCom; SC) was assessed *in vitro* across five SynComs (SC1 to SC5) and *in planta* across 2 SynComs (SCA and CSB) **(A)**. The phylogenetic relationships of the selected bacterial strains, the prevalence in 740 seed samples (Simonin et al., 2022), the associated T6SS clusters and the distribution in SynComs are depicted in **(B)**. SynComs were designed with different phylogenetic diversity (**C**) and T6SS richness (**D**).

RESULTS

T6SS prevalence among seed-associated bacteria

In order to build SynComs with different levels of T6SS diversity, we sequenced 180 bacterial genomes isolated from radish, bean and rapeseed seeds and seedlings (**Table S1**). Among these 180 genomes 61.7% (111 genomes) possess at least one T6SS cluster (**Fig. 2**). T6SS is detected in all bacterial families analyzed, except for genomes of monoderms (e.g. *Bacillaceae*, *Paenibacillaceae*, *Microbacteriaceae* and *Nocardioidaceae*), which do not contain diderm-like protein secretion systems (54). Most T6SS clusters (n=229) belong to T6SS subtype i (n=226), while subtype iii was restricted to the Bacteroidetes families *Weeksellaceae* (n=1) and *Flavobacteriaceae* (n=2). Among T6SS subtype i, the following groups were detected: i1 (n=57), i2 (n=63), i3 (n=80), i4a (n=1), i4b (n=21), i5 (n=4). Seed-associated bacteria possess on average 1.6 T6SS clusters per genome with a range of 1 to 5 clusters per genome. Overall, T6SS is highly prevalent among seed-associated bacteria and might play a significant role for the colonization of the seed habitat.

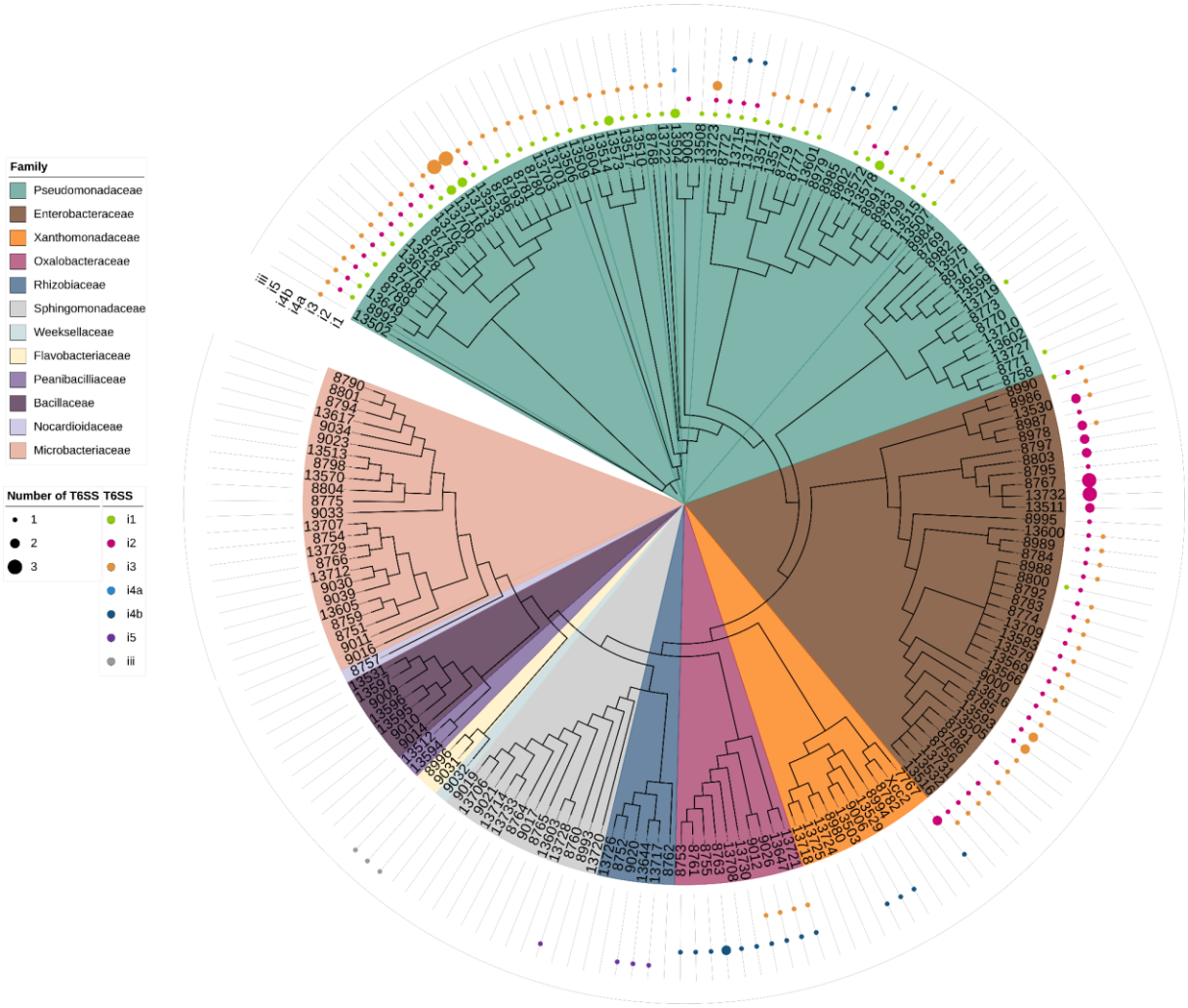

Figure 2. T6SS distribution among seed-associated bacteria. Maximum likelihood (PhyML) phylogenetic tree was constructed using 24 marker genes from a dataset of 180 genomes of seed-associated bacterial strains of rapeseed, radish and bean. Bacteria are color-coded according to their phylogenetic families. T6SS clusters are colored according to their classification, which was determined through an analysis of the conserved TssB protein. The sizes of the shapes correspond to the number of T6SS belonging to a specific group present in the bacterial genomes.

S. rhizophila CFBP13503 T6SS shapes the structure of bacterial SynComs *in vitro*

To analyze the impact of a T6SS secretion system on the assembly of bacterial communities associated with seeds, we chose a strain of *S. rhizophila*, CFBP13503, whose T6SS is capable of inhibiting the growth of *X. campestris* pv. *campestris* (Xcc) under *in vitro* conditions (33). We constructed 5 SynComs with contrasting levels of observed phylogenetic diversity (Faith's PD, **Fig. 1C**) and T6SS richness (**Fig. 1D**). These SynComs were either inoculated with the wild-type (WT) strain CFBP13503 or with an isogenic mutant deleted for its T6SS (Δ*hcp*). After 6 and 24 hours of confrontation in TSA10% media, the composition of these SynComs was evaluated by amplicon sequencing.

Of the 3,233,153 reads obtained after sequence processing, 99.5% corresponded to the *gyrB* sequences of the inoculated strains. In terms of sensitivity, 42 strains out of the 47 inoculated were detected in at least one time point. Confrontations between SynComs and CFBP13503 strains (WT or *Δhcp*) significantly ($P < 0.001$) impacted the phylogenetic composition (weighted UniFrac distance) of all SynComs, explaining 26% to 75% of variance (**Table S3**). A significant increase ($P < 0.05$) in Shannon diversity index was observed from time 6h for almost all SynComs (with the exception of SC3) when communities were inoculated with Δ*hcp* (**Fig. 3A**). The magnitude of this increase in alpha-diversity was greater at 24 h, except once again for SC3. Phylogenetic diversity of SynCom did not explain changes in Shannon diversity since SynComs with equivalent levels of phylogenetic (e.g. SC3 and SC5) responded differently to the T6SS of *S. rhizophila* CFBP13503 (**Fig. 3A**).

Given that some T6SS are specifically activated when bacteria are attacked by T6SS or bacterial competitors (55, 56), the impact of T6SS richness in SynCom composition was investigated. We hypothesized that some strains with T6SSs will respond to the attack of *S. rhizophila* CFBP13503 and therefore will have no or moderate changes in relative abundance. According to our results the number of T6SS per community was not correlated with this change in alpha diversity level (**Fig. 3A**).

Changes in relative abundance of SynCom members were observed when interacting with CFBP13503 strains (**Fig. S1**). A decrease in relative abundance of strains affiliated to *Pseudomonadaceae*, *Enterobacteriaceae*, and *Xanthomonadaceae* was observed during confrontation with the WT (**Fig. 4A**). In contrast, relative abundance of strains belonging to *Bacillaceae*, *Microbacteriaceae*, and *Rhizobiaceae* were enriched when inoculated with the WT (**Fig. 4A**). Overall, these results indicate that the T6SS of *S. rhizophila* CFBP13503 targets a wide range of phylogenetically distinct taxonomic groups.

By comparing relative abundance of SynComs members at 6h and their cophenetic distances with CFBP13503 we detected a significant correlation (P = 0.002) explaining 25% of the observed variance (**Fig. 3B**). This relationship could be explained by a greater metabolic overlap for strains closer to *S. rhizophila* CFBP13503. Indeed, an inverse correlation (R^2 = 0.26, P = 0.001) between changes in relative abundance of SynCom members and resource overlap with CFBP13503 was observed at 6h (**Fig. 3C**). At 24h, none of these correlations were significant (**Fig. S2**) due to probable other competition mechanisms and second order interactions in SynComs.

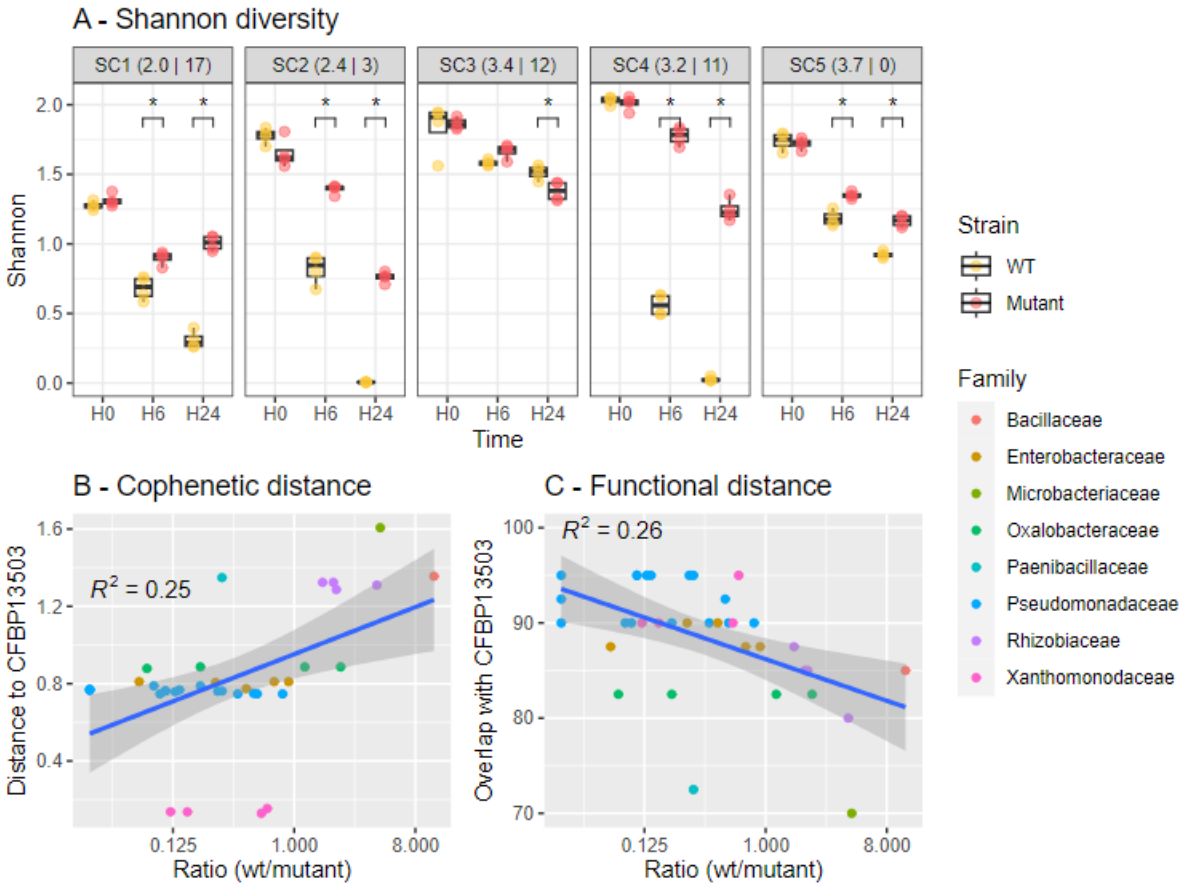

Figure 3. T6SS of *S. rhizophila* CFBP13503 modulated SynCom diversity.

(A) Shannon diversity of bacterial communities during confrontations with *S. rhizophila* CFBP13503 wild type (WT) and the isogenic T6SS mutant *Δhcp* at different time points (0h, 6h and 24h). The phylogenetic diversity (Faith's index) and number of T6SS clusters per SynCom are indicated in parentheses. **(B)** Correlation between changes in relative abundance of SynCom members at 6h and their cophenetic distances to CFBP13503**. (C)** Correlation between changes in relative abundance of SynCom members at 6h and their resource overlap with CFBP13503.

The T6SS of *S. rhizophila* CFBP13503 inhibits the growth of a wide range of bacteria

Pairwise confrontation assays between CFBP13503 strains and rifampicin-resistant variants of 20 selected SynCom members were performed to validate the observed changes in relative abundance detected with *gyrB* amplicon sequencing (**Fig. 4A**). The data obtained with these confrontation assays at 6h were in agreement with the estimated relative abundance for 17 of the 20 strains tested (**Fig. 4A** and **Fig. 4B, Table S1**). The three strains with conflicting data were all enriched in relative abundance within SynComs but were sensitive to the T6SS of CFBP13503 according to CFU count in pairwise confrontations assays. These strains belong to *Plantibacter* (CFBP13513) and *Oxalobacteraceae* (CFBP8753 and CFBP8763). Altogether these results indicate that the relative abundance measured at 6h with *gyrB* amplicon sequencing is a good first approximation for determining whether strains are sensitive or resistant to the T6SS of CFBP13503.

At 6h, the number of CFU of 14 strains was significantly (P <0.05) reduced by the T6SS of CFBP13503 (**Fig. 4B**). At 24 h, almost all tested strains (18 out of 20) were significantly (P <0.05) affected (**Fig. 4C**). The four additional bacterial members detected after 24 h of confrontation with CFBP13503 strains all belong to the *Rhizobiaceae*.

Although there is a relationship between phylogenetic distance and the intensity of bacterial response to T6SS in CFBP13503, this is only partial and does not apply to all the bacteria targeted in this study. For instance, differences in response amplitude were observed within *Oxalobacteraceae*, where 3 strains (CFBP13647, CFBP8761 and CFBP13708) were highly altered by the T6SS from *S. rhizophila* CFBP13503, whereas populations of CFBP8753 and CFBP8763 were less impacted even after 24 h of confrontation (**Fig. 4B**). This result demonstrates differences in bacterial sensitivity independently of the phylogenetic distance between prey and predator.

Under our *in vitro* conditions, the T6SS of *S. rhizophila* CFBP13503 does not provide a multiplication or survival advantage, since the population sizes of WT or *Δhcp* were identical for almost all pairwise confrontations at the two times analyzed (**Fig. S3**). However, there are exceptions that allow CFBP13503 to multiply more easily with its T6SS when interacting with *Pantoea agglomerans* or other *Stenotrophomonas* strains (**Fig. S3**).

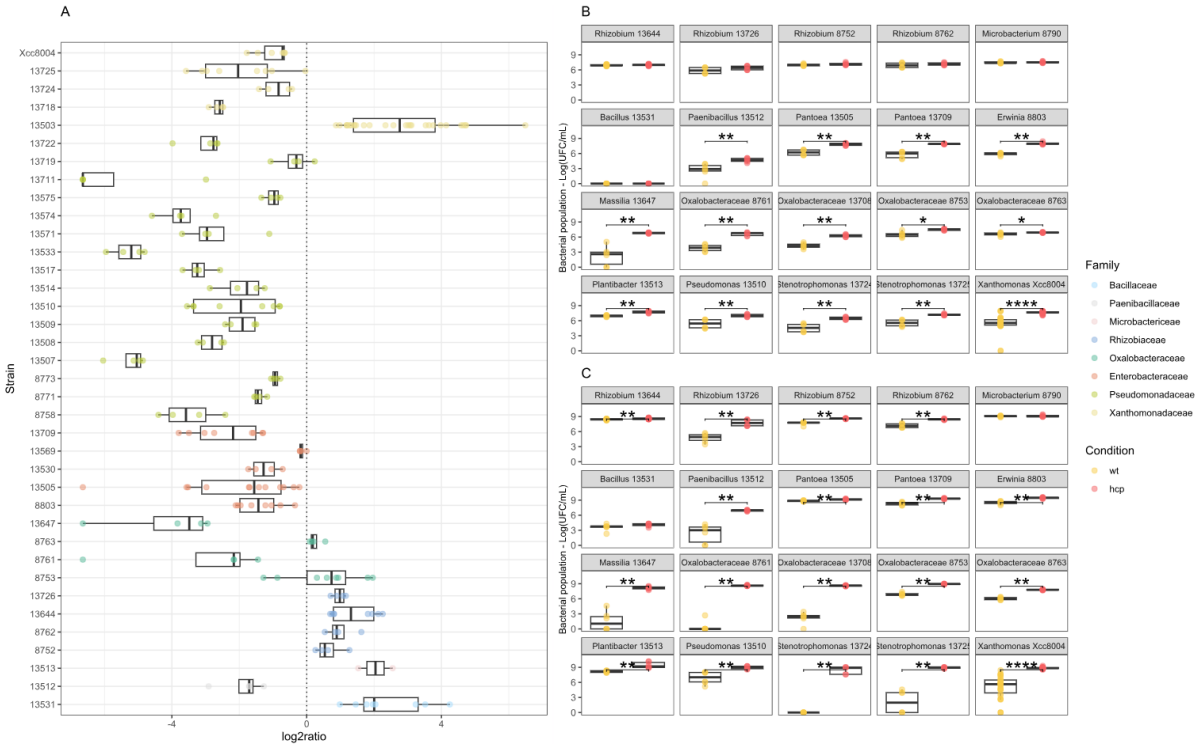

Figure 4. Strain sensitivity to T6SS-mediated competition of *S. rhizophila* CFBP13503.

The strain relative abundance (log2ratio) between wild type vs *hcp* mutant confrontation in SynComs.The more negative value of log2ratio corresponds to a higher sensitivity to T6SS (**A**). Bacterial populations (CFU.ml^{-1}) of some Rifampicin-resistant strains were monitored after pairwise confrontation with *S. rhizophila* CFBP13503 wild-type or its isogenic T6SS-deficient mutant *Δhcp* in TSA10 medium for 6h (**B**) and 24h (**C**). Colony-forming units (CFU) were quantified on TSA10 supplemented with rifampicin. Six or 15 (Xcc8004) replicates are plotted. Statistical analyses were performed using Wilcoxon-Mann-Whitney Test (* p-value < 0.05; ** p-value <0.01; *** p-value < 0.001; **** p-value < 0.0001).

S. rhizophila CFBP13503 T6SS influences specific bacterial taxa transmission from seed to seedling

The broad host range of the T6SS of *S. rhizophila* CFBP13503 observed *in vitro* questions (i) the role of this system in the seedling transmission capacity of this strain and (ii) its involvement in community assembly in soil microbiome competition context.

Since *S. rhizophila* CFBP13503 is efficiently transmitted to seedlings of radish under gnotobiotic conditions (35), we used this plant species to investigate its T6SS impact on microbiota transmission in living potting soil. We first inoculated seeds with CFBP13503 strains (WT or Δ*hcp*) and collected germinated seeds and seedlings. Under these experimental conditions, we confirmed the efficient transmission of *S. rhizophila* CFBP13503 on germinated seeds (average of 1.6 10^6 cells) and seedlings (aerial: 2.4 10^5 cells, root: 2.2 10^4 cells, **Fig. 5A**). According to *gyrB* amplicon sequencing, CFBP13503 reached 15% (germinated seeds), 11% (seedling - aerial compartment) and 2% (seedling - root compartment) of the relative abundance of bacterial communities (**Fig. 5B**). No significant differences in CFBP13503 population size and relative abundance between WT and Δ*hcp* were detected in all studied habitats (**Fig. 5**), which suggest that the T6SS of this strain is not involved in seed-to-seedling transmission.

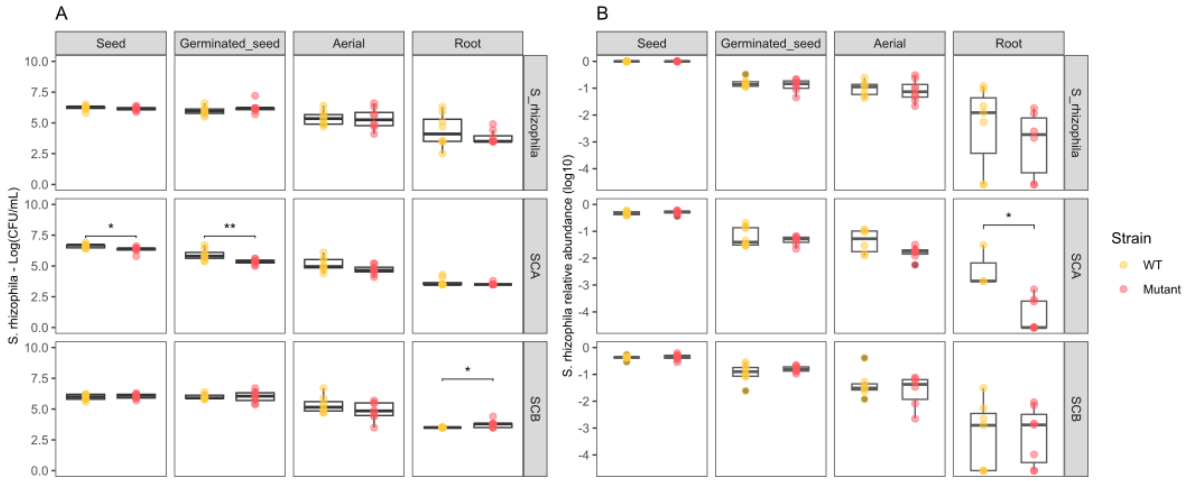

Figure 5 : Abundance of *S. rhizophila* CFBP13503 during seed to seedling transmission. (**A**) *S. rhizophila* CFBP13503 populations were enumerated on selective media (TSA10+Spe^{50}+Amp^{100}) media. The colors represent the inoculated *S. rhizophila* CFBP13503 strain WT (yellow) and Δhcp (red). Data are plotted as CFU / individual. **(B)** Relative abundance of *S. rhizophila* CFBP13503 according to *gyrB* amplicon sequencing . Statistical analysis were performed using Wilcoxon-Mann-Whitney test (* p-value < 0.05).

The high inoculation of CFBP13503 populations (10^6 CFU per seed) within the native seed communities, generally around 10^3 per seed, could explain why no effect of interference

competition by T6SS could be demonstrated. A second experiment was therefore carried out through seed-inoculation of CFBP13503 strains (WT or Δ*hcp*) into two distinct synthetic communities (SCA and SCB). These two communities differ not only in Faith's phylogenetic diversity (SCA: 1.9; SCB : 2.8) but also in their composition of T6SS-susceptible and -resistant strains, with SCA made up solely of susceptible strains and SCB made up of two susceptible strains and two resistant strains (**Table S2**). When CFBP13503 strains were seed-inoculated with SCA (low-diversity community composed of T6SS susceptible strains), T6SS-deficient population sizes were significantly less abundant in seed and germinated-seeds compared to the WT (**Fig. 5A**). Difference in CFBP13503 population size was observed following seed-inoculation with SCB on roots (**Fig. 5A**). By analyzing the relative abundance of SynComs members through *gyrB* amplicon sequencing, 4 strains showed significant ($P < 0.05$) increases in relative abundance at the germinated seed stage (**Fig. 6**). Two of these strains belong to SCA, while the other two from SCB are the two strains previously identified as T6SS-sensitive. These results indicate that some of the strains (4 out of 6) sensitive to the T6SS of *S. rhizophila* CFBP13503 *in vitro* were also sensitive to this secretion system *in planta*. However, this effect is fairly early, since the significant changes in relative abundance were all observed at the germinated seed stage.

As SynCom members represented at best 50% of germinated-seed and seedling communities (**Fig. 6**), the impact of CFBP13503 T6SS on native members of the microbiota (i.e. non-inoculated, soil bacteria) was next investigated. No change in alpha-diversity (Shannon) and beta-diversity (weighted UniFrac distances) was detected. relative abundance of each bacterial taxonomic rank (from phyla to ASV) was compared following inoculation with CFBP13503 WT strain or the T6SS-deficient mutant. We were able to detect very few taxa with significant changes in relative abundance (corrected p-value < 0.05). Only ASVs associated with *Bradyrhizobiaceae* had an increased relative abundance in the presence of the T6SS deficient mutant of CFBP13503 in the root compartment (**Fig. S4**).

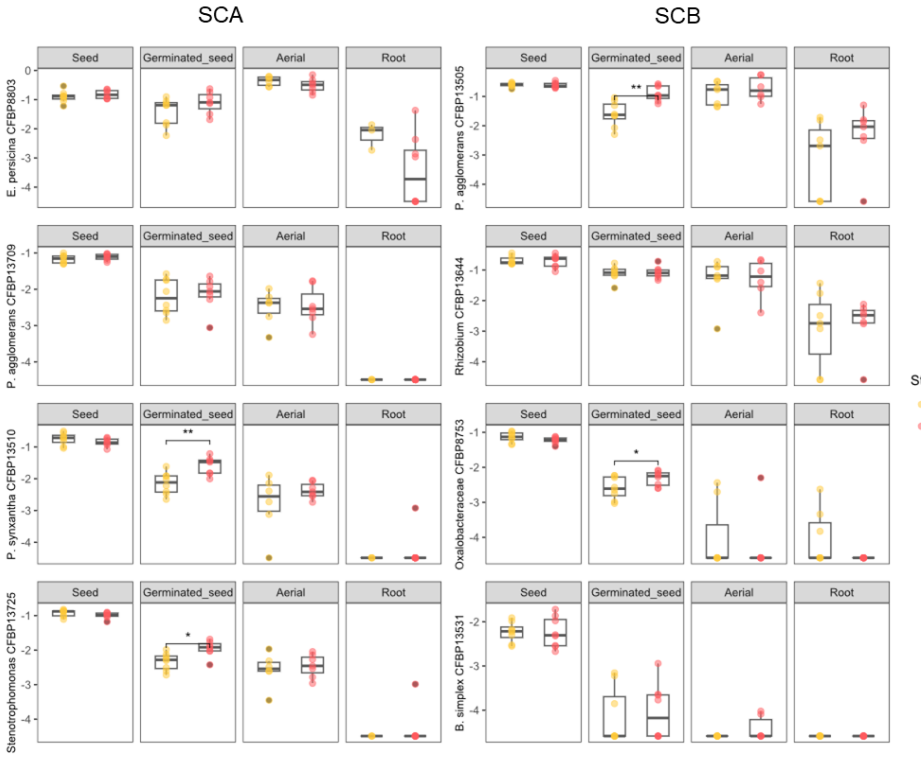

Figure 6. Relative abundance of SynCom members *in planta*. Relative abundance of seed-inoculated bacteria during interaction with *S. rhizophila* CFBP13503 strains (WT or Δ*hcp*). Statistical analysis were performed using Wilcoxon-Mann-Whitney test (* p-value < 0.05).

DISCUSSION

T6SS is highly prevalent among seed-associated bacteria

T6SS is frequently found in Gram-negative bacteria with 17,183 putative T6SS gene clusters detected in 7,617 genomic sequences out of 26,573 as of November 2021 (44). Analysis of a diversity of bacterial strains isolated from radish, rapeseed and bean seed samples showed that 60% of genomic sequences had a T6SS secretion system predominantly affiliated to the T6SS[i]. This percentage rises to 75% when only Proteobacteria are considered, a percentage similar to that previously described above for plant-associated proteobacteria (21).

T6SS of *S. rhizophila* CFBP13503 targets a broad spectrum of bacterial species

The T6SS of *S. rhizophila* CFBP13503, which belongs to cluster i4B, is involved in growth inhibition of the plant pathogen *X. campestris* pv. *campestris* both *in vitro* and *in planta* (33). In the present work, we have demonstrated that this effect is involved in the *in vitro* inhibition of a broad spectrum of seed-borne bacteria belonging to *Enterobacteraceae*, *Xanthomonadaceae*, *Oxalobacteraceae* and *Pseudomonodaceae*. The diversity of prey targeted by a single T6SS is not specific to *S. rhizophila* CFBP13503. For instance, the T6SS i4B of the plant-associated bacterial strains *Pseudomonas putida* KT2440 (57), *Burkholderia gladioli* NGJ1 (58) or *Paraburkholderia sabiae* LMG24235 (59) are involved in inhibition of a range of phytopathogenic agents including *Agrobacterium tumefaciens*, *Pectobacterium carotovorum*, *Pseudomonas syringae*, *Ralstonia solanacearum* and *Xanthomonas campestris*.

The phylogenetic proximity of bacterial prey to *S. rhizophila* CFBP13503 partly explains their susceptibility to its T6SS.

Interference competition mediated through T6SS-contact dependent mechanisms was more prevalent among phylogenetically similar species. Moreover, according to predictions of resource acquisition pathways from bacterial strain genomes, the closer bacteria are to *S. rhizophila* CFBP13503, the more likely they are to be susceptible to its T6SS. These relationships were only observed for 6h confrontations. These early effects could be due to rapid TssB sheath contraction and firing (60) because of the small size of TssA in *S. rhizophila* (354 aa) compared to that of *P. aeruginosa* (518 aa). In multispecies biofilms, the confrontation of *P. putida* KT2440 with soil communities revealed similar results, where

metabolic similarities led to an enhancement of T6SS antimicrobial activity (61). Taken together, these observations indicate that resource overlap drives only in part the evolution of T6SS-mediated interbacterial competition in a manner analogous to that observed for contact-independent inhibition (32).

Immunity-dependent versus-independent mechanisms

The inhibition of a wide range of prey species by *S. rhizophila* T6SS could be explained by its large predicted T6SS effector repertoire (n=9), which cover a large variety of potential activities including phospholipases, amidases, pore-forming effectors and DNases (33). The concomitant delivery of a cocktail of effectors can provide a bet-hedging strategy to promote bacterial competitiveness in the face of unpredictable and variable environmental (62) like during transmission from seed to seedling. Given the generic nature of these activities, it is interesting to understand why certain bacterial families are sensitive while others are resistant. It is highly probable that the resistance of strains to the T6SS of CFBP13503 is related to immunity-independent mechanisms (30). For instance, several monoderm strains tested in this work are resistant to the T6SS of CFBP13503. This resistance could be explained by the thick peptidoglycan layer of monoderms, which requires specific T6SS effectors to be perforated (63, 64) or the induction of survival mechanisms such as sporulation, which has been observed in *B. subtilis* in response to the secretion of a muramidase-type effector secreted by *P. chlororaphis* (65). Concerning *Oxalobacteraceae*, while certain strains exhibit resistance within the communities, they paradoxically show susceptibility when individually confronted with *S. rhizophila* CFBP13503. The varied responses of *Oxalobacteraceae* could be attributed to collective protection within communities. This type of protection has been observed in *E. coli*, where the secretion of exopolysaccharides (EPS) serves to shield unproductive EPS strains from the T6SS of *Acinetobacter baylyi* (66). Another explanation could be the existence of immunity genes in some targeted bacteria that protect from some toxical T6SS effectors (T6Es) of *S. rhizophila* CFBP1350. Such hypotheses will be investigated by looking for putative interactions between T6Es and immunity proteins from surrounding bacteria.

SynComs response to T6SS in CFBP13503 not explained by T6SS richness

T6SS can be assembled in different ways from random firing (e.g. *Vibrio cholerae* (67)) to specific response to T6SS attack (e.g. *Pseudomonas aeruginosa* (55)). The T6SS i4B of *S.*

rhizophila CFBP13503 possesses an ortholog of TslA (33), a periplasmic protein involved in T6SS assembly at the site of contact between neighboring cells (68). Hence it is likely that the T6SS of *S. rhizophila* CFBP13503 is activated during contact with prey cells in our *in vitro* confrontation assays. By defining synthetic communities with different T6SS diversity, we anticipated a response from T6SS-positive strains that have notably a tit-for-tat strategy (i.e. some *Pseudomonas* strains with a T6SS i3). This response should ultimately limit the competitive advantage of CFBP13503 in these T6SS-positive communities. According to *gyrB* amplicon sequencing, the richness and diversity of T6SS in SynComs were not correlated to CFBP13503 relative abundance. Several factors may explain this observation, including the high ratio of CFBP13503 in relation to the preys, a large spectrum of immunity against other bacteria T6SS effectors or the T6SS systems of the other bacterial competitors might not be actively functioning under *in vitro* conditions. Indeed, the T6SS is a tightly regulated mechanism, with its expression being responsive to an array of biotic and/or abiotic factors (69–71).

T6SS impact on bacterial community assembly during seed to seedling transmission depends on the inoculated SynCom composition on seed

We investigated how *S. rhizophila* CFBP13503 T6SS impacts bacterial community dynamics during seed-to-seedling transmission, aiming to observe bacteria responses within their natural environment. The inoculation of bacterial SynComs is the most reliable way to homogenize seed colonization compared to the highly variable single seed microbiota (7, 72). Using *gyrB* metabarcoding, we tracked the transmission of two synthetic communities and soil-associated bacteria across various stages of plant development, encompassing seeds, germinated seeds, and seedlings. The different SynCom members successfully colonized the seeds, resulting in distinct community compositions at the seed stage. However, a convergence in community composition was detected upon seed germination, which reflects a preferential colonization of this habitat by soil-borne taxa as already observed in rapeseed and wheat (5, 8). While the T6SS of *S. rhizophila* CFBP13503 was not an important driver of whole community composition, changes in relative abundances of SynCom members in germinating seeds and some soil-borne taxa (i.e. *Bradyrhizobiaceae*) in roots were detected. The impact of T6SS on the relative abundance of susceptible inoculated strains resulted in an increase in the population and relative abundance of *S. rhizophila* CFBP13503, demonstrating that T6SS can provide a competitive advantage depending on the susceptibility of bacterial

competitors. However, a subset of SynCom members (CFBP13709, CFBP8803, and CFBP8753) remained unaffected. This disparity in response could be attributed to the contrasting environments of *in vitro* confrontation assays, where direct cell-to-cell contact occurs within a confined space, and the more complex spatial dynamics introduced by seed germination and plant growth. The intricate nature of seed germination and plant growth introduces substantial spatial disruptions, a phenomenon demonstrated to increasingly favor sensitive strains that can evade contact with T6SS-producing cells (73). Furthermore, to discern the direct impacts of T6SS on a bacterial member, co-localization is essential (74). Only specific plant habitats may be affected by the T6SS of competitors as it was demonstrated for the gallobiome of tomato induced by *Agrobacterium*, but only during summer time of gall development (75). The precise nature of the impact of *S. rhizophila* T6SS on individual bacterial taxa, whether direct or indirect, remains to be determined. Nonetheless, our study elucidates a clear pattern: while T6SS exerts a negative and specific impact on certain bacterial taxa, it simultaneously creates a favorable environment for other taxa. These changes in bacterial taxa distribution have cascading effects on bacterial interactions, resulting in distinct community dynamics.

ACKNOWLEDGEMENTS

This work was funded by the TypeSEEDS project (INRAE: Plant Health and Environment division, HoloFlux Metaprogram) and the Region des Pays de la Loire (RFI “Objectif Végétal”). We thank the CIRM- CFBP for providing access to strains of their culture collection.

REFERENCES

1. Simonin M, Briand M, Chesneau G, Rochefort A, Marais C, Sarniguet A, Barret M. 2022. Seed microbiota revealed by a large-scale meta-analysis including 50 plant species. New Phytologist 234:1448–1463.

2. Shade A, Jacques M-A, Barret M. 2017. Ecological patterns of seed microbiome diversity, transmission, and assembly. Current Opinion in Microbiology 37:15–22.

3. Johnston-Monje D, Gutiérrez JP, Lopez-Lavalle LAB. 2021. Seed-transmitted bacteria and fungi dominate juvenile plant microbiomes. Front Microbiol 12:737616.

4. Kim H, Jeon J, Lee KK, Lee Y-H. 2022. Longitudinal transmission of bacterial and fungal communities from seed to seed in rice. 1. Commun Biol 5:1–14.

590 5. Rochefort A, Simonin M, Marais C, Guillerm-Erckelboudt A-Y, Barret M, Sarniguet A. 2021.
591 transmission of seed and soil microbiota to seedling. mSystems 6:e0044621.

592 6. Yang L, Danzberger J, Schöler A, Schröder P, Schloter M, Radl V. 2017. Dominant groups of
593 potentially active bacteria shared by barley seeds become less abundant in root associated
594 microbiome. Front Plant Sci 8.

595 7. Arnault G, Marais C, Préveaux A, Briand M, Poisson A-S, Sarniguet A, Barret M, Simonin M.
596 2024. Seedling microbiota engineering using bacterial synthetic community inoculation on
597 seeds. FEMS Microbiology Ecology 100:fiae027.

598 8. Walsh CM, Becker-Uncapher I, Carlson M, Fierer N. 2021. Variable influences of soil and seed-
599 associated bacterial communities on the assembly of seedling microbiomes. 9. ISME J 15:2748–
600 2762.

601 9. Nelson EB. 2004. Microbial dynamics and interactions in the spermosphere. Annu Rev
602 Phytopathol 42:271–309.

603 10. Olofintila OE, Noel ZA. 2023. Soybean and cotton spermosphere soil microbiome shows
604 dominance of soilborne copiotrophs. Microbiology Spectrum 11:e00377-23.

605 11. Darrasse A, Darsonval A, Boureau T, Brisset M-N, Durand K, Jacques M-A. 2010. Transmission of
606 plant-pathogenic bacteria by nonhost seeds without induction of an associated defense
607 reaction at emergence. Appl Environ Microbiol 76:6787–6796.

608 12. Ortega-Cuadros M, De Souza TL, Berruyer R, Aligon S, Pelletier S, Renou J-P, Arias T, Campion C,
609 Guillemette T, Verdier J, Grappin P. 2022. Seed transmission of pathogens: non-canonical
610 immune response in *Arabidopsis* germinating seeds compared to early seedlings against the
611 necrotrophic fungus *Alternaria brassicicola*. 13. Plants 11:1708.

612 13. Granato ET, Meiller-Legrand TA, Foster KR. 2019. The evolution and ecology of bacterial
613 warfare. Current Biology 29:R521–R537.

614 14. Koch AL. 2001. Oligotrophs versus copiotrophs. Bioessays 23:657–661.

615 15. Barret M, Briand M, Bonneau S, Préveaux A, Valière S, Bouchez O, Hunault G, Simoneau P,
616 Jacques M-A. 2015. Emergence shapes the structure of the seed microbiota. Appl Environ
617 Microbiol 81:1257–1266.

618 16. Torres-Cortés G, Bonneau S, Bouchez O, Genthon C, Briand M, Jacques M-A, Barret M. 2018.
619 Functional microbial features driving community assembly during seed germination and
620 emergence. Front Plant Sci 9.

621 17. Allsopp LP, Bernal P, Nolan LM, Filloux A. 2020. Causalities of war: the connection between type
622 VI secretion system and microbiota. Cell Microbiol 22:e13153.

623 18. Pukatzki S, Ma AT, Revel AT, Sturtevant D, Mekalanos JJ. 2007. Type VI secretion system
624 translocates a phage tail spike-like protein into target cells where it cross-links actin.
625 Proceedings of the National Academy of Sciences 104:15508–15513.

626 19. Barret M, Egan F, Fargier E, Morrissey JP, O'Gara F. 2011. Genomic analysis of the type VI
627 secretion systems in *Pseudomonas spp.*: novel clusters and putative effectors uncovered.
628 Microbiology (Reading) 157:1726–1739.

629 20. Bayer-Santos E, Ceseti L de M, Farah CS, Alvarez-Martinez CE. 2019. Distribution, function and
630 regulation of type 6 secretion systems of *Xanthomonadales*. Front Microbiol 10.

631 21. Bernal P, Llamas MA, Filloux A. 2018. Type VI secretion systems in plant-associated bacteria.
632 Environ Microbiol 20:1–15.

633 22. Boyer F, Fichant G, Berthod J, Vandenbrouck Y, Attree I. 2009. Dissecting the bacterial type VI
634 secretion system by a genome wide in silico analysis: what can be learned from available
635 microbial genomic resources? BMC Genomics 10:104.

636 23. de Bruin OM, Ludu JS, Nano FE. 2007. The *Francisella* pathogenicity island protein IglA localizes
637 to the bacterial cytoplasm and is needed for intracellular growth. BMC Microbiol 7:1.

638 24. Clemens DL, Ge P, Lee B-Y, Horwitz MA, Zhou ZH. 2015. Atomic structure of T6SS reveals
639 interlaced array essential to function. Cell 160:940–951.

640 25. Russell AB, Wexler AG, Harding BN, Whitney JC, Bohn AJ, Goo YA, Tran BQ, Barry NA, Zheng H,
641 Peterson SB, Chou S, Gonen T, Goodlett DR, Goodman AL, Mougous JD. 2014. A type VI
642 secretion-related pathway in Bacteroidetes mediates interbacterial antagonism. Cell Host &
643 Microbe 16:227–236.

644 26. Böck D, Medeiros JM, Tsao H-F, Penz T, Weiss GL, Aistleitner K, Horn M, Pilhofer M. 2017. *In*
645 *situ* architecture, function, and evolution of a contractile injection system. Science 357:713–
646 717.

647 27. Allsopp LP, Bernal P. 2023. Killing in the name of: T6SS structure and effector diversity.
648 Microbiology 169:001367.

649 28. Hood RD, Singh P, Hsu F, Güvener T, Carl MA, Trinidad RRS, Silverman JM, Ohlson BB, Hicks KG,
650 Plemel RL, Li M, Schwarz S, Wang WY, Merz AJ, Goodlett DR, Mougous JD. 2010. A type VI
651 secretion system of *Pseudomonas aeruginosa* targets a toxin to bacteria. Cell Host Microbe
652 7:25–37.

653 29. Ross BD, Verster AJ, Radey MC, Schmidtke DT, Pope CE, Hoffman LR, Hajjar AM, Peterson SB,
654 Borenstein E, Mougous JD. 2019. Human gut bacteria contain acquired interbacterial defense
655 systems. 7781. Nature 575:224–228.

656 30. Hersch SJ, Manera K, Dong TG. 2020. Defending against the type six secretion system: beyond
657 immunity genes. 2. Cell Reports 33:108259.

31. Robitaille S, Trus E, Ross BD. 2021. Bacterial defense against the type VI secretion system. Trends Microbiol 29:187–190.

32. Russel J, Røder HL, Madsen JS, Burmølle M, Sørensen SJ. 2017. Antagonism correlates with metabolic similarity in diverse bacteria. PNAS 114:10684–10688.

33. Garin T, Brin C, Préveaux A, Brault A, Briand M, Simonin M, Barret M, Journet L, Sarniguet A. 2024. The type VI secretion system of *Stenotrophomonas rhizophila* CFBP13503 limits the transmission of *Xanthomonas campestris* pv. *campestris* 8004 from radish seeds to seedlings. Molecular Plant Pathology 25:e13412.

34. Torres-Cortés G, Garcia BJ, Compant S, Rezki S, Jones P, Préveaux A, Briand M, Roulet A, Bouchez O, Jacobson D, Barret M. 2019. Differences in resource use lead to coexistence of seed-transmitted microbial populations. 1. Sci Rep 9:1–13.

35. Simonin M, Préveaux A, Marais C, Garin T, Arnault G, Sarniguet A, Barret M. 2023. Transmission of synthetic seed bacterial communities to radish seedlings: impact on microbiota assembly and plant phenotype. Peer Community Journal 3.

36. Armanhi JSL, de Souza RSC, de Araújo LM, Okura VK, Mieczkowski P, Imperial J, Arruda P. 2016. Multiplex amplicon sequencing for microbe identification in community-based culture collections. Sci Rep 6:29543.

37. Luo R, Liu B, Xie Y, Li Z, Huang W, Yuan J, He G, Chen Y, Pan Q, Liu Y, Tang J, Wu G, Zhang H, Shi Y, Liu Y, Yu C, Wang B, Lu Y, Han C, Cheung DW, Yiu S-M, Peng S, Xiaoqian Z, Liu G, Liao X, Li Y, Yang H, Wang J, Lam T-W, Wang J. 2012. SOAPdenovo2: an empirically improved memory-efficient short-read de novo assembler. GigaSci 1:18.

38. Zerbino DR, Birney E. 2008. Velvet: Algorithms for de novo short read assembly using de Bruijn graphs. Genome Res 18:821–829.

39. Seah B. 2016. phylogenomics-tools: First release (v0.1). Zenodo.

40. Wu M, Scott AJ. 2012. Phylogenomic analysis of bacterial and archaeal sequences with AMPHORA2. Bioinformatics 28:1033–1034.

41. Stamatakis A. 2014. RAxML version 8: a tool for phylogenetic analysis and post-analysis of large phylogenies. Bioinformatics 30:1312–1313.

42. Letunic I, Bork P. 2021. Interactive Tree Of Life (iTOL) v5: an online tool for phylogenetic tree display and annotation. Nucleic Acids Research 49:W293–W296.

43. Karaoz U, Brodie EL. 2022. microTrait: A toolset for a trait-based representation of microbial genomes. Front Bioinform 2.

44. Zhang J, Guan J, Wang M, Li G, Djordjevic M, Tai C, Wang H, Deng Z, Chen Z, Ou H-Y. 2023. SecReT6 update: a comprehensive resource of bacterial Type VI Secretion Systems. Sci China Life Sci 66:626–634.

693 45. Martin M. 2011. Cutadapt removes adapter sequences from high-throughput sequencing reads.
694 1. EMBnet.journal 17:10–12.

695 46. Callahan BJ, McMurdie PJ, Rosen MJ, Han AW, Johnson AJA, Holmes SP. 2016. DADA2: High-
696 resolution sample inference from Illumina amplicon data. 7. Nat Methods 13:581–583.

697 47. Frøslev TG, Kjøller R, Bruun HH, Ejrnæs R, Brunbjerg AK, Pietroni C, Hansen AJ. 2017. Algorithm
698 for post-clustering curation of DNA amplicon data yields reliable biodiversity estimates. Nat
699 Commun 8:1188.

700 48. Wang Q, Garrity GM, Tiedje JM, Cole JR. 2007. Naïve Bayesian Classifier for Rapid Assignment of
701 rRNA Sequences into the New Bacterial Taxonomy. Applied and Environmental Microbiology
702 73:5261–5267.

703 49. Davis NM, Proctor DM, Holmes SP, Relman DA, Callahan BJ. 2018. Simple statistical
704 identification and removal of contaminant sequences in marker-gene and metagenomics data.
705 Microbiome 6:226.

706 50. McMurdie PJ, Holmes S. 2013. Phyloseq: an R package for reproducible interactive analysis and
707 graphics of microbiome census data. PLOS ONE 8:e61217.

708 51. Lozupone C, Knight R. 2005. UniFrac: a new phylogenetic method for comparing microbial
709 communities. Applied and Environmental Microbiology 71:8228–8235.

710 52. Barnett DJ m, Arts IC w, Penders J. 2021. microViz: an R package for microbiome data
711 visualization and statistics. Journal of Open Source Software 6:3201.

712 53. Martin BD, Witten D, Willis AD. 2020. Modeling microbial abundances and dysbiosis with beta-
713 binomial regression. Ann Appl Stat 14.

714 54. Abby SS, Cury J, Guglielmini J, Néron B, Touchon M, Rocha EPC. 2016. Identification of protein
715 secretion systems in bacterial genomes. 1. Sci Rep 6:23080.

716 55. Basler M, Ho BT, Mekalanos JJ. 2013. Tit-for-Tat: type VI secretion system counterattack during
717 bacterial cell-cell interactions. Cell 152:884–894.

718 56. Kamal F, Liang X, Manera K, Pei T-T, Kim H, Lam LG, Pun A, Hersch SJ, Dong TG. 2020.
719 Differential cellular response to translocated toxic effectors and physical penetration by the
720 type VI secretion system. Cell Reports 31:107766.

721 57. Bernal P, Allsopp LP, Filloux A, Llamas MA. 2017. The *Pseudomonas putida* T6SS is a plant
722 warden against phytopathogens. 4. The ISME Journal 11:972–987.

723 58. Yadav SK, Magotra A, Ghosh S, Krishnan A, Pradhan A, Kumar R, Das J, Sharma M, Jha G. 2021.
724 Immunity proteins of dual nuclease T6SS effectors function as transcriptional repressors. EMBO
725 Rep 22:e51857.

726 59. Hug S, Heiniger B, Bolli K, Paszti S, Eberl L, Ahrens CH, Pessi G. 2023. *Paraburkholderia sabiae*
727 uses one type VI secretion system (T6SS-1) as a powerful weapon against notorious plant
728 pathogens. Microbiology Spectrum 11:e01622-23.

729 60. Bernal P, Furniss RCD, Fecht S, Leung RCY, Spiga L, Mavridou DAI, Filloux A. 2021. A novel
730 stabilization mechanism for the type VI secretion system sheath. Proceedings of the National
731 Academy of Sciences 118:e2008500118.

732 61. Xiong X, Wan W, Ding B, Cai M, Lu M, Liu W. 2024. Type VI secretion system drives bacterial
733 diversity and functions in multispecies biofilms. Microbiological Research 279:127570.

734 62. LaCourse KD, Peterson SB, Kulasekara HD, Radey MC, Kim J, Mougous JD. 2018. Conditional
735 toxicity and synergy drive diversity among antibacterial effectors. 4. Nature Microbiology
736 3:440–446.

737 63. Le N-H, Pinedo V, Lopez J, Cava F, Feldman MF. 2021. Killing of Gram-negative and Gram-
738 positive bacteria by a bifunctional cell wall-targeting T6SS effector. Proceedings of the National
739 Academy of Sciences 118:e2106555118.

740 64. Pei T-T, Kan Y, Wang Z-H, Tang M-X, Li H, Yan S, Cui Y, Zheng H-Y, Luo H, Liang X, Dong T. 2022.
741 Delivery of an Rhs-family nuclease effector reveals direct penetration of the gram-positive cell
742 envelope by a type VI secretion system in Acidovorax citrulli. mLife 1:66–78.

743 65. Pérez-Lorente AI, Molina-Santiago C, de Vicente A, Romero D. 2023. Sporulation activated via
744 σW protects *Bacillus* from a Tse1 peptidoglycan hydrolase T6SS effector. Microbiol Spectr
745 11:e0504522.

746 66. Granato ET, Smith WPJ, Foster KR. 2023. Collective protection against the type VI secretion
747 system in bacteria. 7. ISME J 17:1052–1062.

748 67. Basler M, Pilhofer M, Henderson GP, Jensen GJ, Mekalanos JJ. 2012. Type VI secretion requires
749 a dynamic contractile phage tail-like structure. 7388. Nature 483:182–186.

750 68. Lin L, Capozzoli R, Ferrand A, Plum M, Vettiger A, Basler M. 2022. Subcellular localization of
751 Type VI secretion system assembly in response to cell–cell contact. The EMBO Journal
752 41:e108595.

753 69. Bernal P, Civantos C, Pacheco-Sánchez D, Quesada JM, Filloux A, Llamas MA. 2023.
754 Transcriptional organization and regulation of the *Pseudomonas putida* K1 type VI secretion
755 system gene cluster. Microbiology 169:001295.

756 70. Hespanhol JT, Nóbrega-Silva L, Bayer-Santos E. 2023. Regulation of type VI secretion systems at
757 the transcriptional, posttranscriptional and posttranslational level. Microbiology 169:001376.

758 71. Marchi M, Boutin M, Gazengel K, Rispe C, Gauthier J-P, Guillerm-Erckelboudt A-Y, Lebreton L,
759 Barret M, Daval S, Sarniguet A. 2013. Genomic analysis of the biocontrol strain *Pseudomonas*
760 *fluorescens* Pf29Arp with evidence of T3SS and T6SS gene expression on plant roots. Environ
761 Microbiol Rep 5:393–403.

762 72. Chesneau G, Laroche B, Préveaux A, Marais C, Briand M, Marolleau B, Simonin M, Barret M.
763 2022. Single seed microbiota: assembly and transmission from parent plant to seedling. mBio
764 13:e01648-22.

765 73. Steinbach G, Crisan C, Ng SL, Hammer BK, Yunker PJ. 2020. Accumulation of dead cells from
766 contact killing facilitates coexistence in bacterial biofilms. 173. Journal of The Royal Society
767 Interface 17:20200486.

768 74. Lin YL, Smith SN, Kanso E, Septer AN, Rycroft CH. 2023. A subcellular biochemical model for
769 T6SS dynamics reveals winning competitive strategies. PNAS Nexus 2:pgad195.

770 75. Wang S-C, Chen A-P, Chou S-J, Kuo C-H, Lai E-M. 2023. Soil inoculation and blocker-mediated
771 sequencing show effects of the antibacterial T6SS on agrobacterial tumorigenesis and
772 gallobiome. mBio 14:e00177-23.

773

SUPPLEMENTARY DATA

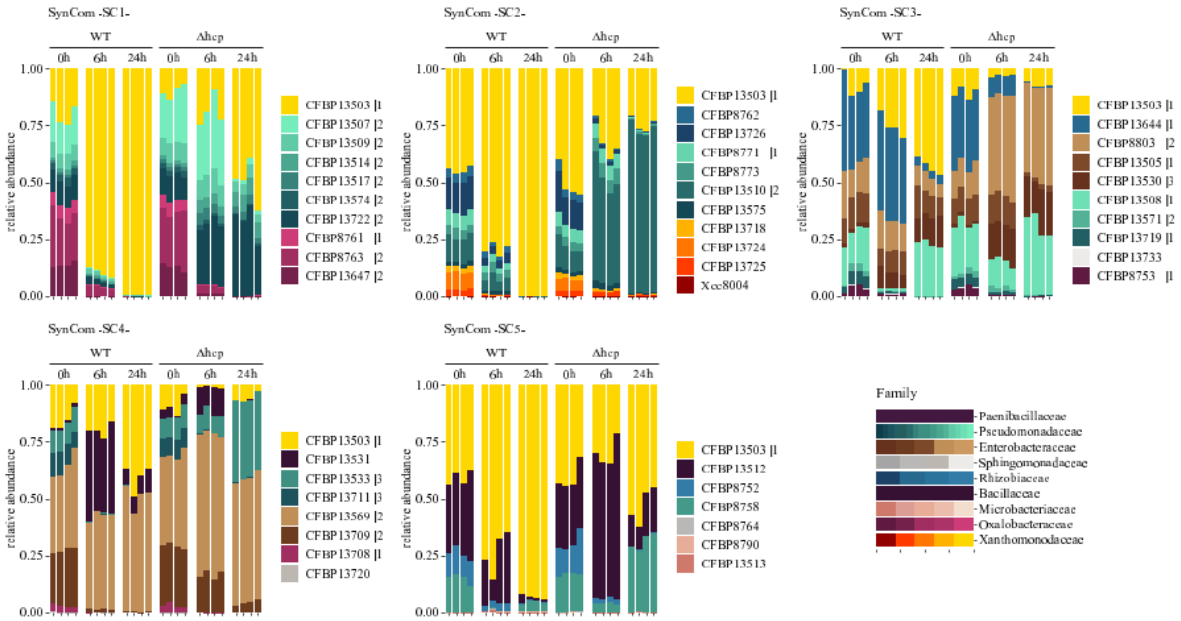

Figure S1. T6SS impact on the structure of bacterial synthetic communities *in vitro*.

Relative abundance of bacterial taxa within five different synthetic communities (SynCom) at different confrontation times (0h, 6h, and 24h) while competing with the wild-type strain of *S. rhizophila* CFBP13503 (WT) or the T6SS-deficient mutant Δ*hcp*. The code number of each strain is followed by its amount of T6SS clusters.

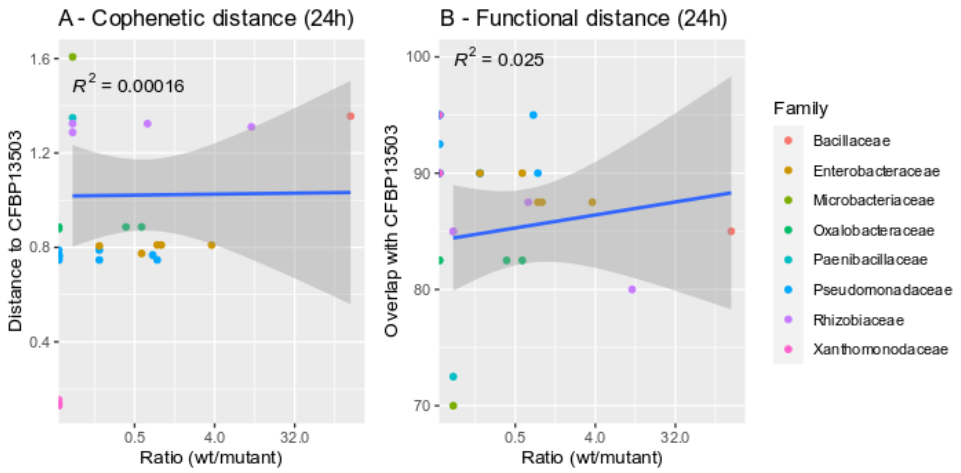

2

Figure S2 Relationship between phylogenetic/functional distances and RA at 24h confrontation of SynCom members. (A) Correlation between changes in relative abundance of SynCom members at 24h and their cophenetic distances to CFBP13503**. (B)** Correlation between changes in relative abundance of SynCom members at 24h and their resource overlap with CFBP13503.

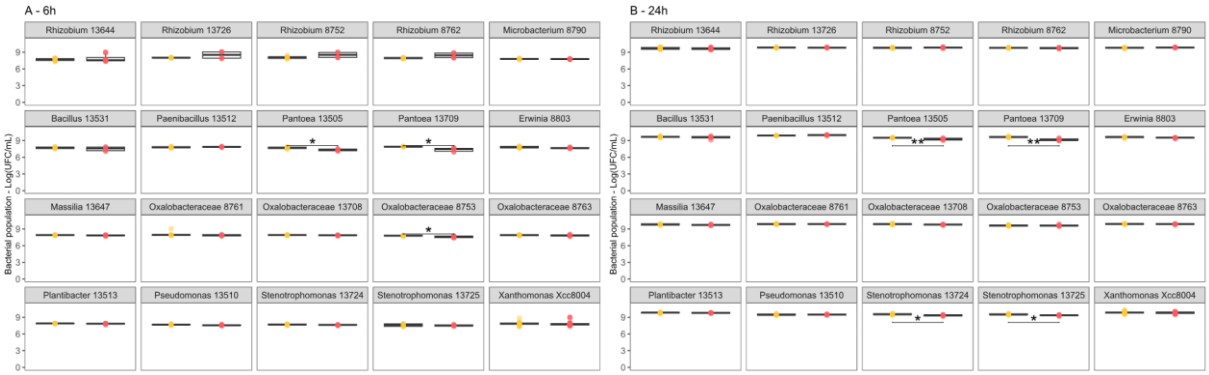

Figure S3. Population dynamics of *S. rhizophila* CFBP13503 and T6SS-deficient mutant *Δhcp* during confrontation with seed-borne bacterial strains. *S. rhizophila* populations (CFU.ml^{-1}) were monitored after confrontation with rifampicin-resistant strains in TSA10 medium for 6h (A) and 24h (B). Colony-forming units (CFU) were quantified on TSA10 supplemented with spectinomycin and ampicillin. Six replicates are plotted. Statistical analyses were performed using Wilcoxon-Mann-Whitney Test (* p-value < 0.05).

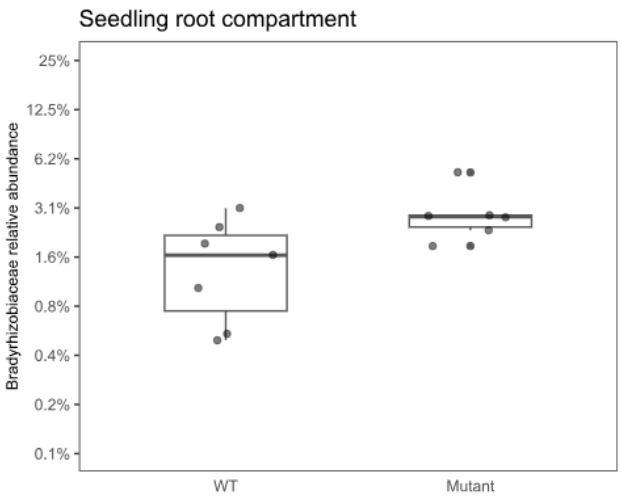

Figure S4. Relative abundance of ASVs affiliated to *Bradyrhizobiaceae* in roots following seed-inoculations of *S. rhizophila* CFBP13503 strains (wt or T6SS-deficient mutant).

Table S1. Investigation of T6SS presence within genome sequences of seed and seedling-associated bacterial strains. *(large table visible in supplementary Table S1)*

Table S2. Strains used to build the different SynComs in this study

Strain	Taxonomy	Biosample	Host	Habitat	Freq (Simonin et al. 2022)	T6SS	I1	I2	I3	I4b	I5	SC1	SC2	SC3	SC4	SC5	SCA	SCB	SC1_fitness (6h)	SC2_fitness (6h)	SC3_fitness (6h)	SC4_fitness (6h)	SC5_fitness (6h)	SCA_fitness (6h)	SCB_fitness (6h)	ratio CFU (6h)	Phenotype (6h)	ratio CFU (24h)	Phenotype (24h)
CFBP13507	Pseudomonas viridiflava	SAMN09062491	Raphanus sativus Flamboyant5	Seed	0,70	2	1	-	1	-	-	1	-	-	-	-	-	-	0,03	-	-	-	-	-	-	-	-	-	-
CFBP13647	Massilia	SAMN16237783	B.napus Tenor	Seed	0,01	2	-	-	1	1	-	1	-	-	-	-	-	-	0,08	-	-	-	-	-	-	-15,24	S	-21,96	S
CFBP13574	Pseudomonas syringae group	SAMN16237900	Raphanus sativus Flamboyant5	Seed	0,41	2	1	-	1	-	-	1	-	-	-	-	-	-	0,09	-	-	-	-	-	-	-	-	-	-
CFBP13517	Pseudomonas fluorescens subgroup	SAMN09064884	Raphanus sativus Flamboyant5	Seed	0,38	2	1	-	1	-	-	1	-	-	-	-	-	-	0,11	-	-	-	-	-	-	-	-	-	-
CFBP13722	Pseudomonas fluorescens subgroup	SAMN16237190	B.napus Boston	Seed	0,19	2	1	-	1	-	-	1	-	-	-	-	-	-	0,13	-	-	-	-	-	-	-	-	-	-
CFBP8761	Oxalobacteraceae	SAMN16237762	B.napus Tenor	Seed	0,00	1	-	-	-	1	-	1	-	-	-	-	-	-	0,20	-	-	-	-	-	-	-9,22	S	-27,20	S
CFBP13509	Pseudomonas fluorescens subgroup	SAMN09062824	Raphanus sativus Flamboyant5	Seed	0,19	2	1	-	1	-	-	1	-	-	-	-	-	-	0,27	-	-	-	-	-	-	-	-	-	-
CFBP13514	Pseudomonas fluorescens subgroup	SAMN09063676	Raphanus sativus Flamboyant5	Seed	0,13	2	1	-	1	-	-	1	-	-	-	-	-	-	0,29	-	-	-	-	-	-	-	-	-	-
Xcc8004	Xanthomonas campestris pv. campestri	SAMN07207934	Brassica oleracea var. botrytis	Leaf	0,27	0	-	-	-	-	-	1	1	1	1	1	-	-	0,63	0,45	nd	nd	nd	-	-	-7,07	S	-12,75	S
CFBP8763	Oxalobacteraceae	SAMN16237778	B.napus Tenor	Seed	0,06	2	-	-	-	2	-	1	-	-	-	-	-	-	1,20	-	-	-	-	-	-	-1,13	S	-5,81	S
CFBP13503	Stenotrophomonas rhizophila	SAMN09064466	Raphanus sativus Flamboyant5	Seed	0,36	1	-	-	-	1	-	1	1	1	1	1	1	1	2,68	2,67	30,47	12,38	2,30	25,48	8,35	-		-	-
CFBP13709	Pantoea agglomerans	SAMN16237131	B.napus Astrid	Seed	0,68	2	-	1	1	-	-	-	-	-	1	-	1	-	-	-	-	0,07	-	0,37	-	-7,16	S	-3,27	S
CFBP13510	Pseudomonas fluorescens subgroup	SAMN09062823	Raphanus sativus Flamboyant5	Seed	0,04	2	1	-	1	-	-	-	1	-	-	-	1	-	-	0,11	-	-	-	0,51	-	-5,45	S	-6,83	S
CFBP13725	Stenotrophomonas	SAMN16237356	B.napus Colvert	Seed	0,21	0	-	-	-	-	-	-	1	-	-	-	1	-	-	0,12	-	-	-	0,56	-	-5,58	S	-22,71	S
CFBP8803	Erwinia persicina	SAMN16237911	Raphanus sativus Flamboyant5	Flower	0,30	2	-	2	-	-	-	-	-	1	-	-	1	-	-	-	0,26	-	-	0,57	-	-6,98	S	-3,17	S
CFBP13508	Pseudomonas koreensis subgroup	SAMN09062492	Raphanus sativus Flamboyant5	Seed	0,06	1	1	-	-	-	-	-	-	1	-	-	-	-	-	-	0,14	-	-	-	-	-	-	-	-
CFBP13505	Pantoea agglomerans	SAMN09062489	Raphanus sativus Flamboyant5	Seed	0,88	1	-	-	1	-	-	-	-	1	-	-	-	1	-	-	0,71	-	-	-	0,35	-5,41	S	-1,00	S
CFBP8758	Pseudomonas putida group	SAMN16237690	B.napus Major	Seed	0,34	0	-	-	-	-	-	-	-	-	-	1	-	-	-	-	-	-	0,10	-	-	-	-	-	-
CFBP13512	Paenibacillus	SAMN09063421	Raphanus sativus Flamboyant5	Seed	0,38	0	-	-	-	-	-	-	-	-	-	1	-	-	-	-	-	-	0,29	-	-	-6,72	S	-15,31	S
CFBP8752	Rhizobium	SAMN16237344	B.napus Boston	Seed	0,00	0	-	-	-	-	-	-	-	-	-	1	-	-	-	-	-	-	1,63	-	-	-0,55	R	-3,06	S
CFBP13513	Plantibacter	SAMN09063410	Raphanus sativus Flamboyant5	Seed	0,35	0	-	-	-	-	-	-	-	-	-	1	-	-	-	-	-	-	4,38	-	-	-2,57	S	-4,26	S
CFBP13533	Pseudomonas orientalis	SAMN16237857	Raphanus sativus Flamboyant5	Seed	0,09	3	1	1	1	-	-	-	-	-	1	-	-	-	-	-	-	0,03	-	-	-	-	-	-	-
CFBP13711	Pseudomonas	SAMN16237133	B.napus Avisо	Seed	0,01	3	1	1	-	1	-	-	-	-	1	-	-	-	-	-	-	0,03	-	-	-	-	-	-	-
CFBP13569	Pantoea agglomerans	SAMN16237903	Raphanus sativus Flamboyant5	Seed	0,56	2	-	1	1	-	-	-	-	-	1	-	-	-	-	-	-	0,91	-	-	-	-	-	-	-
CFBP13531	Bacillus simplex	SAMN16237854	Raphanus sativus Flamboyant5	Seed	0,00	0	-	-	-	-	-	-	-	-	1	-	-	1	-	-	-	11,01	-	-	3,02	nd	nd	-1,58	R
CFBP13571	Pseudomonas syringae group	SAMN16237876	Raphanus sativus Flamboyant5	Seed	0,24	2	1	-	1	-	-	-	-	1	-	-	-	-	-	-	0,20	-	-	-	-	-	-	-	-
CFBP13530	Enterobacter cancerogenus	SAMN09064920	Raphanus sativus Flamboyant5	Seed	0,07	3	-	2	1	-	-	-	-	1	-	-	-	-	-	-	0,44	-	-	-	-	-	-	-	-
CFBP13719	Pseudomonas putida group	SAMN16237175	B.napus Boston	Seed	0,07	1	1	-	-	-	-	-	-	1	-	-	-	-	-	-	0,82	-	-	-	-	-	-	-	-
CFBP8753	Oxalobacteraceae	SAMN16237354	B.napus Boston	Seed	0,01	1	-	-	-	1	-	-	-	1	-	-	-	1	-	-	2,22	-	-	-	1,50	-3,34	S	-6,80	S
CFBP13644	Rhizobium	SAMN16237137	B.napus Avisо	Seed	0,31	1	-	-	-	-	1	-	-	1	-	-	-	1	-	-	4,13	-	-	-	1,70	-0,19	R	-0,55	S
CFBP13718	Stenotrophomonas	SAMN16237142	B.napus Avisо	Seed	0,02	0	-	-	-	-	-	-	1	-	-	-	-	-	-	0,16	-	-	-	-	-	-	-	-	-
CFBP8771	Pseudomonas putida group	SAMN16237697	B.napus Major	Seed	0,06	1	1	-	-	-	-	-	1	-	-	-	-	-	-	0,38	-	-	-	-	-	-	-	-	-
CFBP13575	Pseudomonas coleopterorum	SAMN16237901	Raphanus sativus Flamboyant5	Seed	0,14	0	-	-	-	-	-	-	1	-	-	-	-	-	-	0,50	-	-	-	-	-	-	-	-	-
CFBP8773	Pseudomonas putida group	SAMN16237754	B.napus Mohican	Seed	0,11	0	-	-	-	-	-	-	1	-	-	-	-	-	-	0,53	-	-	-	-	-	-	-	-	-
CFBP13724	Stenotrophomonas	SAMN16237355	B.napus Boston	Seed	0,12	0	-	-	-	-	-	-	1	-	-	-	-	-	-	0,57	-	-	-	-	-	-6,33	S	-28,01	S
CFBP13726	Rhizobium	SAMN16237357	B.napus Colvert	Seed	0,10	0	-	-	-	-	-	-	1	-	-	-	-	-	-	1,96	-	-	-	-	-	-1,69	R	-9,92	S
CFBP8762	Rhizobium	SAMN16237769	B.napus Tenor	Seed	nd	0	-	-	-	-	-	-	1	-	-	-	-	-	-	2,06	-	-	-	-	-	-0,79	R	-4,16	S
CFBP13714	Sphingomonas	SAMN16237136	B.napus Avisо	Seed	0,08	0	-	-	-	-	-	-	-	-	-	1	-	-	-	-	-	-	-	-	-	-	-	-	-
CFBP13729	Frigoribacterium	SAMN16237389	B.napus Colvert	Seed	0,19	0	-	-	-	-	-	-	-	-	1	-	-	-	-	-	-	-	-	-	-	-	-	-	-
CFBP8751	Frigoribacterium	SAMN16237779	B.napus Tenor	Seed	0,02	0	-	-	-	-	-	-	-	-	-	1	-	-	-	-	-	-	-	-	-	-	-	-	-
CFBP8757	Aeromicrobium	SAMN16237654	B.napus Major	Seed	0,01	0	-	-	-	-	-	-	-	-	-	1	-	-	-	-	-	-	-	-	-	-	-	-	-
CFBP8759	Frigoribacterium	SAMN16237713	B.napus Mohican	Seed	0,06	0	-	-	-	-	-	-	-	-	1	-	-	-	-	-	-	-	-	-	-	-	-	-	-
CFBP13733	Sphingomonas	SAMN16237468	B.napus Express	Seed	0,10	0	-	-	-	-	-	-	-	1	-	-	-	-	-	-	nd	-	-	-	-	-	-	-	-
CFBP13708	Oxalobacteraceae	SAMN16237124	B.napus Astrid	Seed	0,02	1	-	-	-	1	-	-	-	-	1	-	-	-	-	-	-	nd	-	-	-	-6,67	S	-21,29	S
CFBP13720	Sphingomonas	SAMN16237345	B.napus Boston	Seed	0,01	0	-	-	-	-	-	-	-	-	1	-	-	-	-	-	-	nd	-	-	-	-	-	-	-
CFBP8764	Sphingomonas	SAMN16237800	B.napus Tenor	Seed	0,09	0	-	-	-	-	-	-	-	-	-	1	-	-	-	-	-	-	nd	-	-	-	-	-	-
CFBP8790	Microbacterium	SAMN16238272	Raphanus sativus Flamboyant5	Seed	0,07	0	-	-	-	-	-	-	-	-	-	1	-	-	-	-	-	-	nd	-	-	-0,20	R	-0,19	R

Table S3. Percentage of variance in bacterial phylogenetic composition of SynCom 1 to 5 (SC1-SC5) explained by initial stains (Strain) composition, time of confrontation (6h and 24h, Time) or Strain xTime interaction

SynCom¤	Strain¤	Time¤	Strain·x·Time¤
SC1¤	36.9¤	30.8¤	ns¤
SC2¤	29.2¤	37.4¤	24.8¤
SC3¤	26.2¤	64.3¤	5.2¤
SC4¤	38.9¤	35.1¤	18.1¤
SC5¤	75.1¤	6.2¤	13.5¤

A

In vitro SynCom confrontation assay

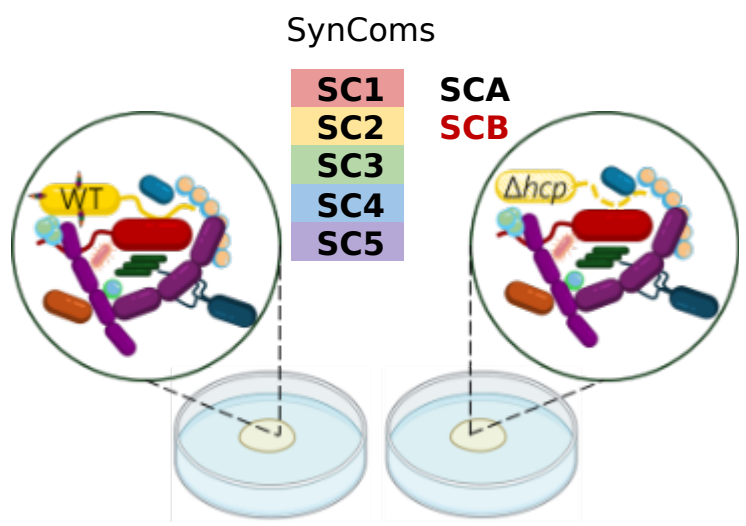

Seed to seedling transmission assay

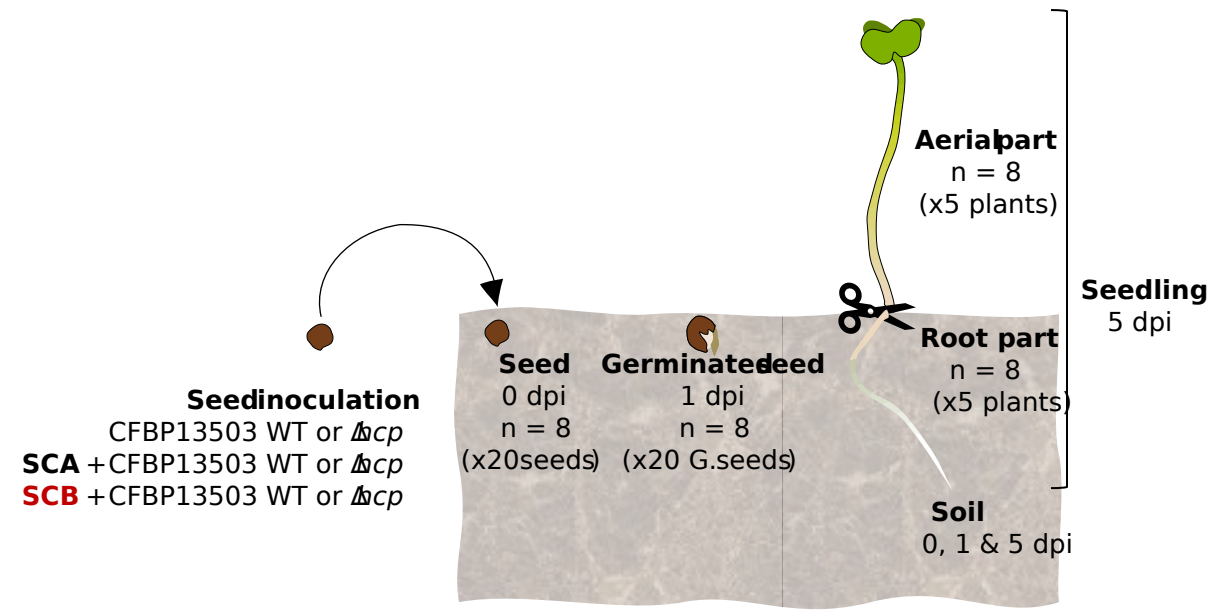

B

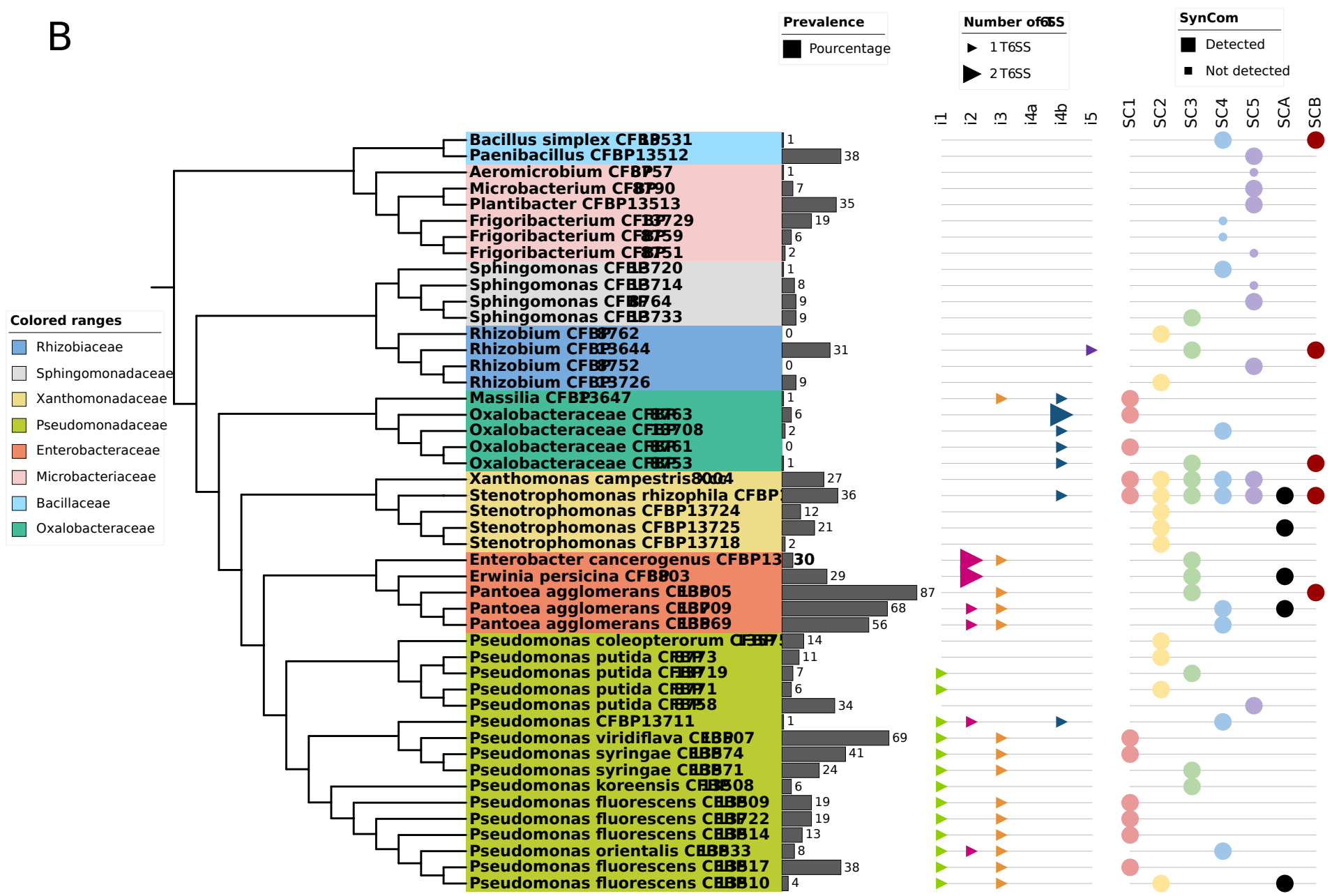

C

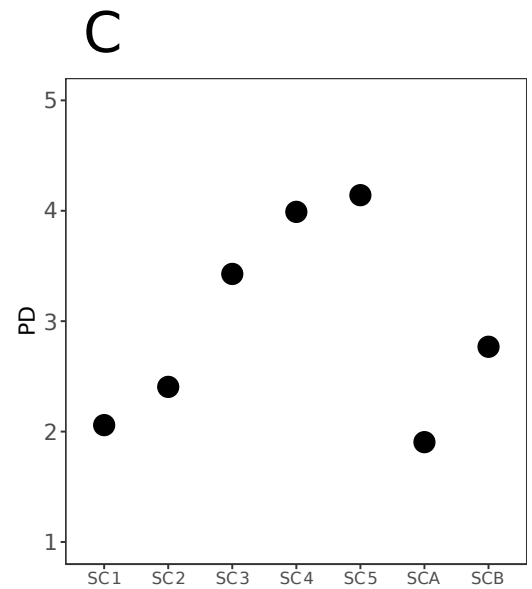

D

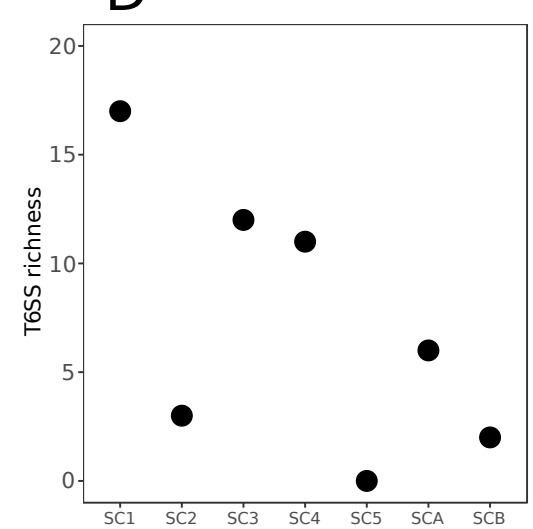

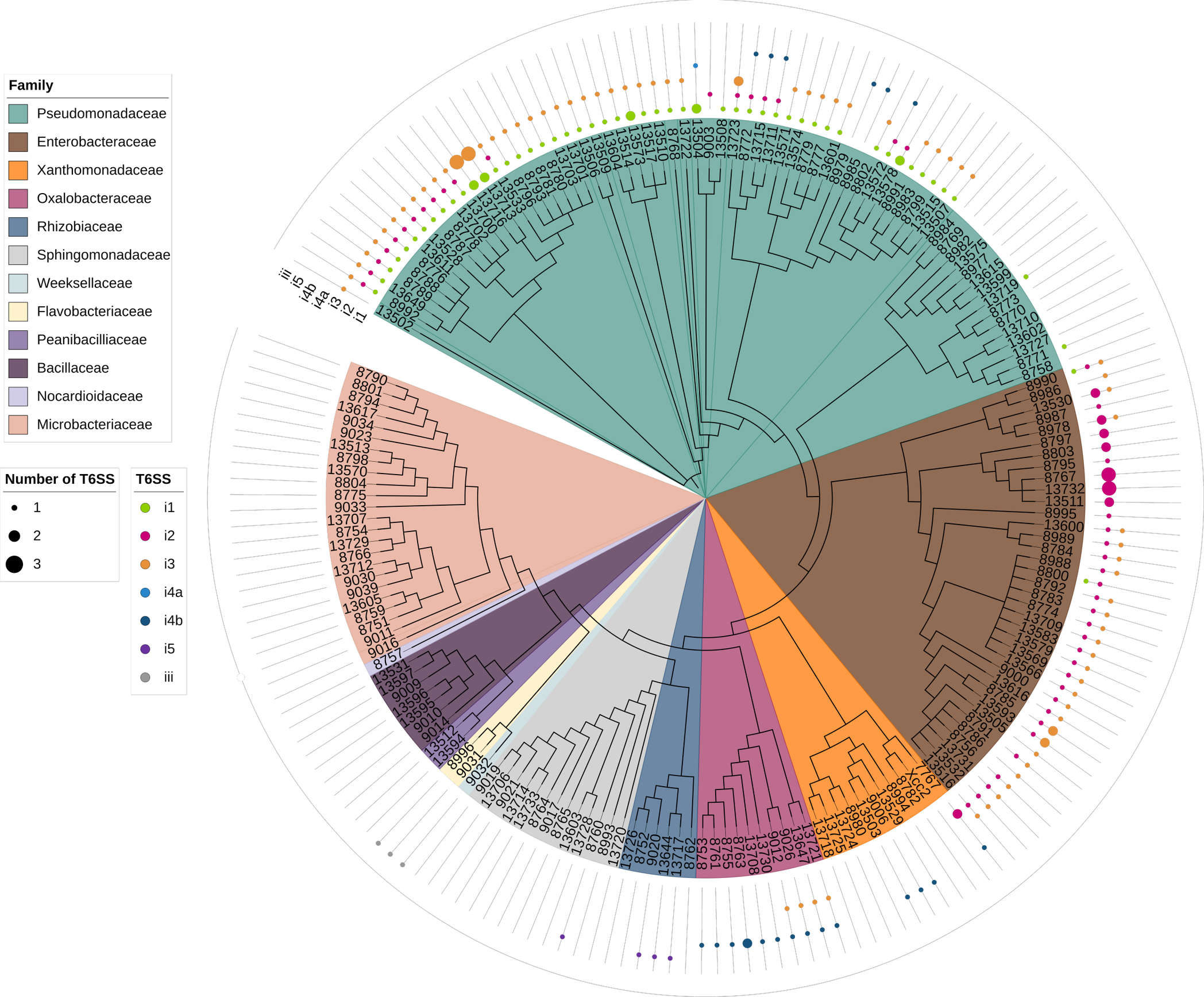
Family
Pseudomonadaceae
Enterobacteraceae
Xanthomonadaceae
Oxalobacteraceae
Rhizobiaceae
Sphingomonadaceae
Weeksellaceae
Flavobacteriaceae
Peanibacilliaceae
Bacillaceae
Nocardioidaceae
Microbacteriaceae
Number of T6SS
1
2
3
T6SS
i1
i2
i3
i4a
i4b
i5
iii

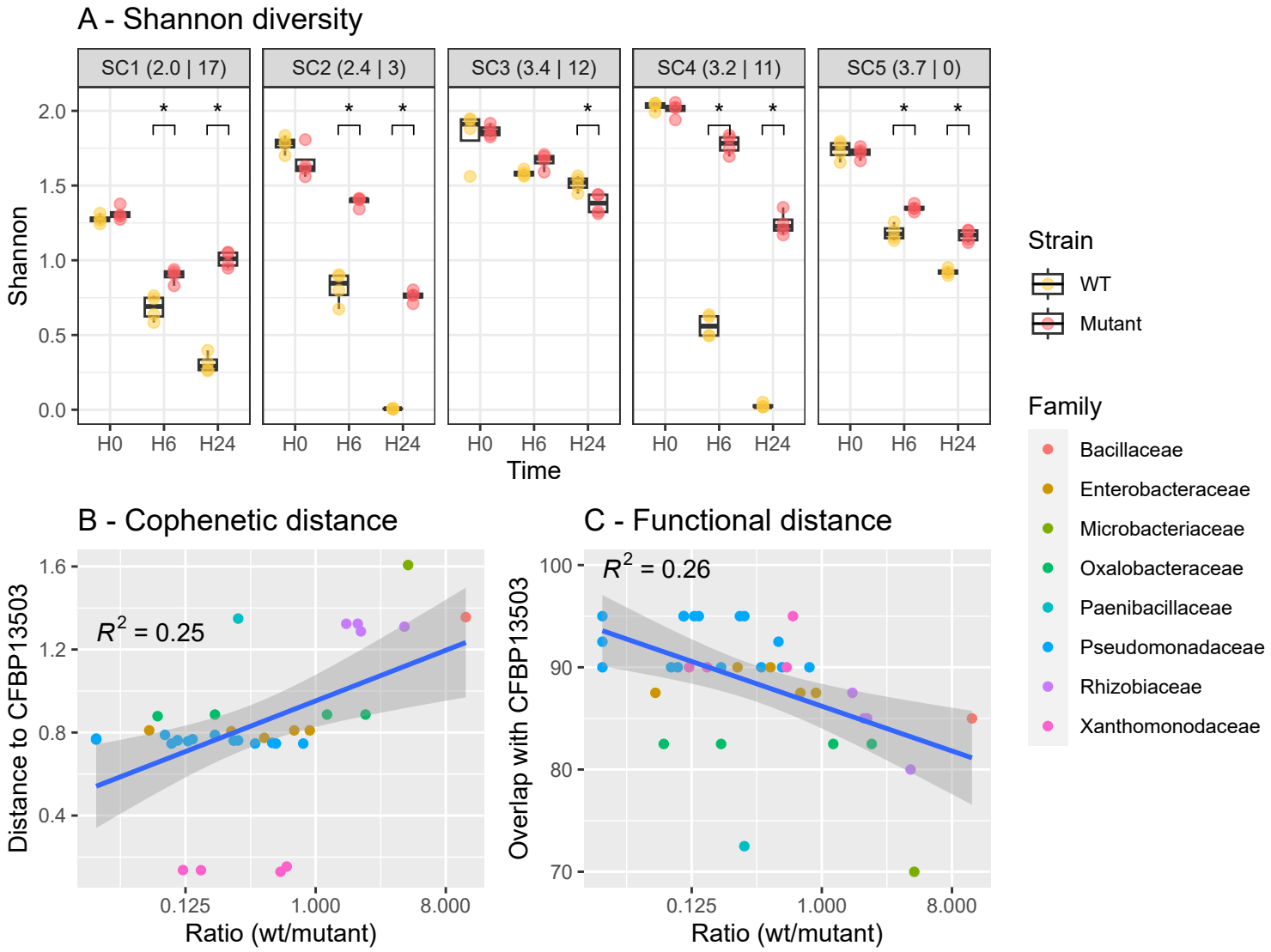
A - Shannon diversity
SC1 (2.0 | 17)
SC2 (2.4 | 3)
SC3 (3.4 | 12)
SC4 (3.2 | 11)
SC5 (3.7 | 0)
Shannon
Time
H0
H6
H24
Strain
WT
Mutant
Family
Bacillaceae
Enterobacteraceae
Microbacteriaceae
Oxalobacteraceae
Paenibacillaceae
Pseudomonadaceae
Rhizobiaceae
Xanthomonodaceae
B - Cophenetic distance
R^2 = 0.25
Distance to CFBP13503
Ratio (wt/mutant)
C - Functional distance
R^2 = 0.26
Overlap with CFBP13503
Ratio (wt/mutant)

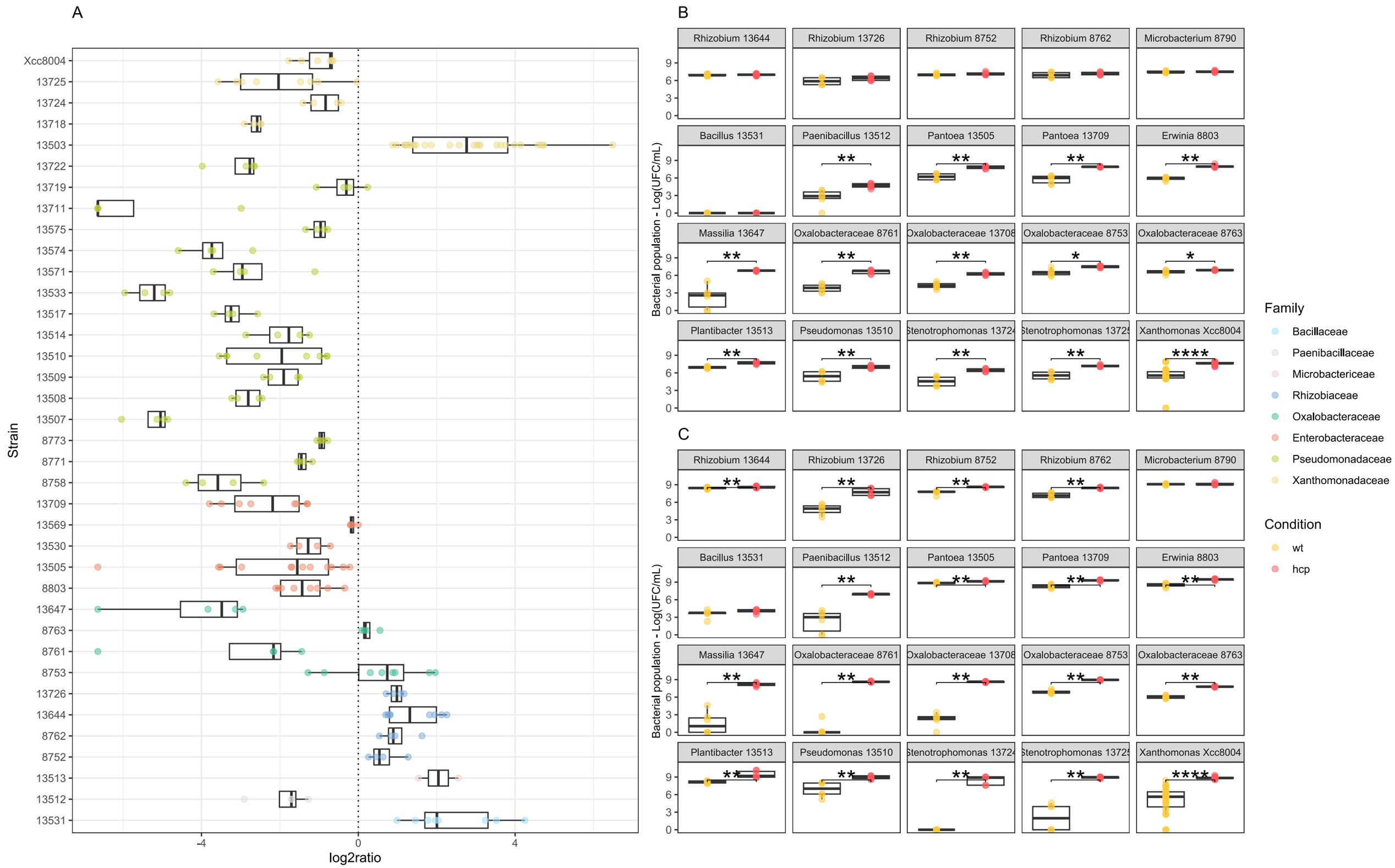
A
Strain
Xcc8004
13725
13724
13718
13503
13722
13719
13711
13575
13574
13571
13533
13517
13514
13510
13509
13508
13507
8773
8771
8758
13709
13569
13530
13505
8803
13647
8763
8761
8753
13726
13644
8762
8752
13513
13512
13531
-4
0
4
log2ratio
B
Rhizobium 13644
Rhizobium 13726
Rhizobium 8752
Rhizobium 8762
Microbacterium 8790
Bacillus 13531
Paenibacillus 13512
Pantoea 13505
Pantoea 13709
Erwinia 8803
Massilia 13647
Oxalobacteraceae 8761
Oxalobacteraceae 13708
Oxalobacteraceae 8753
Oxalobacteraceae 8763
Plantibacter 13513
Pseudomonas 13510
Stenotrophomonas 13724
Stenotrophomonas 13725
Xanthomonas Xcc8004
Bacterial population - Log(UFC/mL)
C
Family
Bacillaceae
Paenibacillaceae
Microbactericeae
Rhizobiaceae
Oxalobacteraceae
Enterobacteraceae
Pseudomonadaceae
Xanthomonadaceae
Condition
wt
hcp

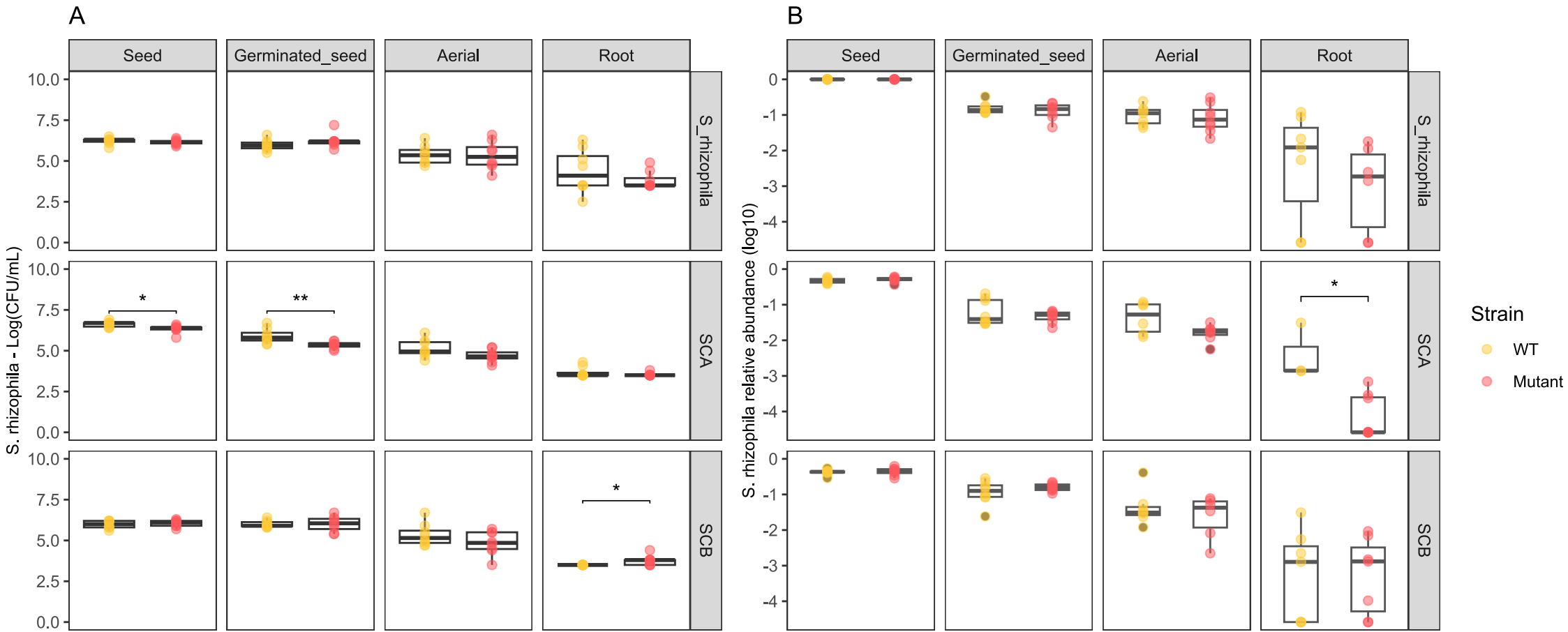
A
B
Seed
Germinated_seed
Aerial
Root
S_rhizophila
SCA
SCB
S. rhizophila - Log(CFU/mL)
S. rhizophila relative abundance (log10)
10.0
7.5
5.0
2.5
0.0
0
-1
-2
-3
-4
*
**
Strain
WT
Mutant

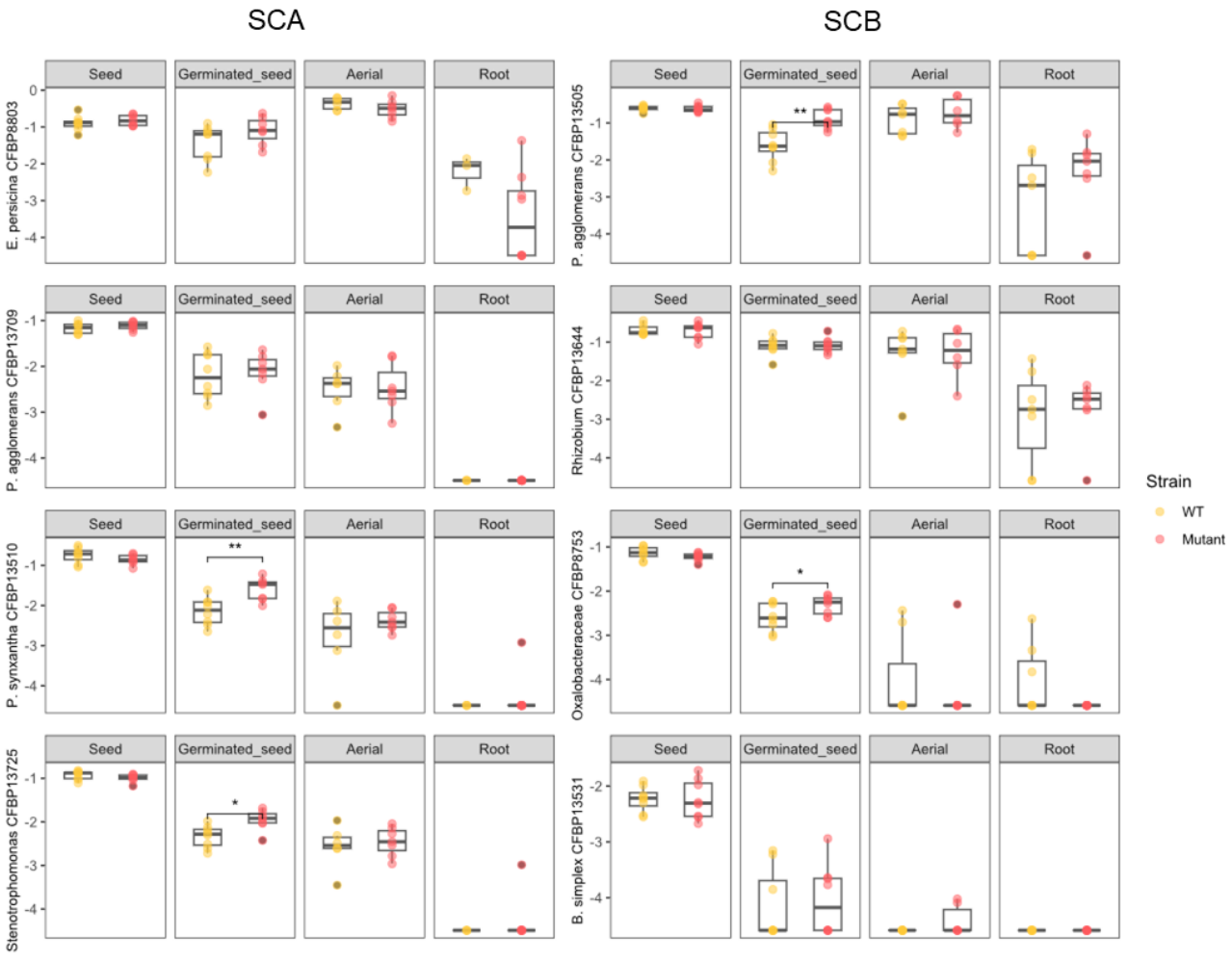
SCA
SCB
Seed
Germinated_seed
Aerial
Root
E. persicina CFBP8803
P. agglomerans CFBP13709
P. synxantha CFBP13510
Stenotrophomonas CFBP13725
P. agglomerans CFBP13505
Rhizobium CFBP13644
Oxalobacteraceae CFBP8753
B. simplex CFBP13531
Strain
WT
Mutant